MOLECULAR, GENETIC, AND CYTOGENETIC ANALYSIS OF THE STRUCTURE AND ORGANIZATION OF THE ABNORMAL CHROMOSOME 10 OF MAIZE

by

REBECCA JEANNE MROCZEK

(Under the Direction of R. Kelly Dawe and Susan R. Wessler)

ABSTRACT

Genetic and molecular mapping, in situ hybridization analysis, and transposon display were used to examine the structure and composition of a meiotic drive system on maize abnormal chromosome 10 (Ab10). The Ab10 chromosome, along with at least 22 other targets of meiotic drive known as knobs, are preferentially transmitted to progeny. Ab10 is thought to promote meiotic drive by transforming knobs into neocentromeres, which move poleward on the spindle such that they are preferentially recovered in female reproductive cells. The Ab10 system is thought to contain at least one inversion that brings the drive loci (genes for trans-acting factors that promote meiotic drive) and the target loci (chromomeres and a large knob on Ab10) into close linkage. A previously reported inversion had not been confirmed at the molecular level, nor had the boundaries of the inversion been established. Genetic mapping was first used to integrate the restriction fragment length polymorphism map (RFLP) and standard genetic maps of the normal 10 chromosome, and then an RFLP map was prepared of the Ab10 chromosome using a set of terminal deficiencies. Comparison of the N10 and Ab10 maps revealed the presence of complex chromosomal rearrangements. Other prior data had established that the Ab10 chromosome contains few essential genes. This, and the fact that recombination is suppressed around inversions, led us to hypothesize that the meiotic drive system may be rich in retroelements and other forms of 'selfish' DNA. This idea was pursued using fluorescent in situ hybridization (FISH) for eight different maize retroelements, and by transposon display for miniature inverted repeat transposable elements (MITEs). The in situ data established that Ab10 itself showed no obvious accumulation of retroelements. However both knobs and centromeres showed a strikingly low abundance of retroelements. Knobs and centromeres are similar in structure and function: both are composed primarily of long repeat arrays and both are known to move on the spindle during cell division. These data suggest that the long repeat arrays in knobs and centromeres are under selection for their role in promoting chromosome movement. Transposon display for MITEs established that they are not unusually abundant on Ab10.

INDEX WORDS: Ab10, retroelements, mapping, in situ hybridization, cytogenetics, maize.

MOLECULAR, GENETIC, AND CYTOGENETIC ANALYSIS OF THE STRUCTURE AND ORGANIZATION OF THE ABNORMAL CHROMOSOME 10 OF MAIZE

by

REBECCA JEANNE MROCZEK

B.A., Boston University, 1997

A Dissertation Submitted to the Graduate Faculty of The University of Georgia in Partial Fulfillment of the Requirements for the Degree

DOCTOR OF PHILOSOPHY

ATHENS, GEORGIA

2003

MOLECULAR, GENETIC, AND CYTOGENETIC ANALYSIS OF THE STRUCTURE AND ORGANIZATION OF THE ABNORMAL CHROMOSOME 10 OF MAIZE

by

REBECCA JEANNE MROCZEK

Major Professors:	R. Kelly Dawe Susan R. Wessler
Committee:	Michael J. Scanlon Wayne Parrott Andrew H. Paterson John McDonald

Electronic Version Approved:

Maureen Grasso
Dean of the Graduate School
The University of Georgia
August 2003

ACKNOWLEDGEMENTS

I would like to thank each of the members of my committee, Dr. Kelly Dawe, Dr. Susan Wessler, Dr. Michael Scanlon, Dr. Wayne Parrott, Dr. Andrew Paterson, and Dr. John McDonald. I would especially like to thank Kelly for his guidance and patience over the course of my graduate studies. I am most grateful to Dr. Marshall Darley, Dr. Susan Wessler, Dr. Norris Armstrong, Dr. Peggy Brickman and Dr. Richard Meagher for providing advice, training, and experience with teaching. I would also like to thank all those in the Dawe lab: Carolyn Lawrence, Juliana Melo, Chris Topp and Dr. Cathy Zhong. I would especially like to thank Juliana Melo for endless work on Southern blots and Dr. Mike Scanlon for providing endless advice. My great appreciation to Carolyn Lawrence for providing valuable assistance with all things computer related, and especially for being a great friend. My great thanks to Dr. Mark Osterlund for his insightful talks, dog walks, and being a truly wonderful friend. I would also like to thank Mike Boyd and Andy Tull at the Plant Biology Department Greenhouse for their wonderful care of my corn. Others that provided valuable help to me during my program include: Dr. John Bowers, Brad Chapman, David Burk, David Henderson, Amy Bouck, and the entire Wessler and Scanlon labs.

My primary support was provided by the NSF Mechanisms of Plant Evolution Training Grant and additional support was provided by RKD's NSF Functional Genomics of Maize Centromeres grant.

My greatest thanks go to my parents Tom and Rachel, my brother Benjamin and my pets Suzie, Envy and Patches for all being there when you were needed most.

TABLE OF CONTENTS

Page

LIST OF TABLES

Page

LIST OF FIGURES

Page

CHAPTER1

INTRODUCTION

The Abnormal Chromosome 10

The Abnormal chromosome 10 of maize (Ab10) is an aberrant form of the normal 10 (N10) chromosome discovered by Longley in a Mexican population of teosinte, the wild relative of maize, and in three populations of maize in the Southwestern United States (LONGLEY 1937; LONGLEY 1938). Ab10 is cytologically distinguishable from the N10 chromosome by a large segment of additional chromatin attached to the long arm of the chromosome (RHOADES 1942; RHOADES and DEMPSEY 1985) (FIGURE 1.1). The additional chromatin is comprised of four regions (FIGURE 1.1): the differential segment which contains three small chromomeres, a euchromatic portion containing an inverted portion of the N10 chromosome, a large heterochromatic knob, and a small euchromatic distal tip (RHOADES and DEMPSEY 1985).

Phenomena associated with Ab10

Shortly after its discovery, genetic studies revealed that Ab10 has three different phenotypes. The first is preferential segregation, or meiotic drive, of the Ab10 chromosome and other knobbed chromosomes to the next generation (KIKUDOME 1959; LONGLEY 1945; RHOADES 1942; RHOADES 1952). Second is the transformation of all heterochromatic knobs into active, centromere-like structures called neocentromeres

(RHOADES 1950; RHOADES 1952; RHOADES and VILKOMERSON 1942). Finally, the Ab10 chromosome causes an increased frequency of recombination in regions that would normally experience reduced recombination due to the presence of structural heterozygosity, such as knobs and inversions (KIKUDOME 1959; RHOADES and DEMPSEY 1966).

Rhoades (1942) first discovered the preferential segregation effect of Ab10 in crosses where Ab10 was marked with the closely linked *R* locus. When r-Ab10/*R*-N10 plants were test-crossed as females to an r-N10 tester, the resulting progeny were approximately 70% r/r instead of the expected, 50% (RHOADES 1942). Rhoades (1942), however, found that the reciprocal cross, where Ab10 was present in the male, resulted in the Ab10 chromosome appearing in less than the expected 50% of the progeny (42-48% Ab10) (RHOADES 1942). These data indicate that Ab10 mediated meiotic drive occurs during female gametogenesis and not during male gametogenesis.

Further analysis of this phenomenon showed that Ab10 also causes the preferential segregation of alleles linked to knobs on chromosomes other than Ab10 (KIKUDOME 1959; LONGLEY 1945; RHOADES and DEMPSEY 1966). For instance, when on a knobbed chromosome 9 the *C*, *Sh*, and *Wx* loci all show preferential segregation in the presence of Ab10 (LONGLEY 1945). It has also been shown that the degree of preferential segregation for a particular locus is dependent upon the distance of the locus from its linked knob; loci that are closer to the knob experience higher degrees of preferential segregation than do loci farther away from the knob (RHOADES and DEMPSEY 1957; RHOADES and DEMPSEY 1966). Additionally, preferential segregation of a knob-

linked locus is dependent upon the size of the knob; larger knobs are preferentially segregated over medium or small knobs (KIKUDOME 1959).

In addition to the preferential segregation of knobs, Ab10 causes the formation of neocentromeres at knobs. Rhoades and Vilkomerson (1942) found that during the two meiotic divisions of microsporogenesis (but not mitosis) secondary sites of centromeric activity, termed neocentromeres, occurred in plants containing the Ab10 chromosome (RHOADES and VILKOMERSON 1942). Neocentromeres were found to occur only on the knobbed homologue of a dyad and resulted in the precocious movement of the knobbed chromatid towards the spindle (RHOADES 1942; RHOADES 1952; RHOADES and VILKOMERSON 1942).

Based upon his observations Rhoades proposed a model for Ab10 mediated meiotic drive that hinges upon the formation of neocentromeres and the occurrence of crossing over between knobbed and non-knobbed homologues (RHOADES 1942; RHOADES 1952). In maize, female meiosis results in a linear tetrad of cells, the basal-most of which is the only cell that develops into a gamete. In Rhoades' model, Ab10 and other knobbed chromosomes are driven to the basal-most cell and ultimately to the egg at frequencies higher than their non-knobbed counterparts, resulting in meiotic drive (FIGURE 1.2). The model requires that recombination between the knobbed and non-knobbed homologues occur in the region between the centromeres and the knobs, producing a heteromorphic dyad. Following recombination, neocentromere activity during meiosis I pulls the knobbed chromatid towards the spindle poles ahead of the centromere and non-knobbed chromatid. The model then requires that the polar orientation of the knobbed chromatid be maintained through interkinesis so that

neocentromere activity during anaphase II results in knobbed chromatids being pulled into the two outer-most cells (RHOADES 1942; RHOADES 1952; RHOADES and DEMPSEY 1966).

Presence of the Ab10 chromosome also causes an increased amount of recombination in regions of structural heterozygosity, such as between knobbed and non-knobbed homologues (KIKUDOME 1959; RHOADES and DEMPSEY 1966). Rhoades and Dempsey (1966) showed a link between recombination and preferential segregation using three different chromosomes, each having varying degrees of crossing over with its homologue: a transposition chromosome 9 carrying a portion of chromosome 3 (Tp9), a rearranged chromosome 9 (the (R)9 chromosome), and three different chromosome 3 inversions (In3a, In3b, and In3c). Their results showed that as the amount of recombination between knobbed and non-knobbed homologues was reduced, preferential segregation was similarly reduced (RHOADES and DEMPSEY 1966), providing strong evidence for the requirement of recombination in preferential segregation.

Organization of the Ab10 chromosome

In attempts to localize the individual functions associated with Ab10, analyses of deficient and rearranged Ab10 chromosomes have been undertaken (EMMERLING 1959; HIATT and DAWE 2003a; MILES 1970; RHOADES and DEMPSEY 1985). Emmerling (1959) demonstrated that loss of the euchromatic distal tip along with either the entire large knob or the distal half of the large knob resulted in loss of preferential segregation. These deficient chromosomes were also associated with an apparent reduction, but not loss, of neocentromere activity (FIGURE 3, K^0 and K^S)(EMMERLING 1959). Additionally, the

recombination effect of Ab10 was mapped to a region proximal to a breakpoint in the proximal one third of the large knob (KV) (MILES 1970). This region was further delimited to be distal to the Df-K breakpoint (HIATT and DAWE 2003a) (FIGURE 1.3).

Rhoades and Dempsey sought to further analyze the organization of Ab10 through the characterization of five Ab10 deficiencies of varying length (FIGURE 1.3, Df-C, Df-I, Df-F, Df-H and Df-K) (RHOADES and DEMPSEY 1972; RHOADES and DEMPSEY 1985). A combination of cytological and genetic analyses of these chromosomes revealed that the *W2*, *O7*, and *L13* genes are in an inverted order on Ab10 relative to N10 such that on Ab10 the gene order is *R*, *L13*, *O7*, *W2*, and *Sr2*. The most severe deficiency, Df-C, has maintained all of the differential segment but is missing nearly all of the inverted region (FIGURE 1.3). These data show that the entire gene-containing segment is separated from the *R* gene by the differential segment (RHOADES and DEMPSEY 1985). These Ab10 deficiencies have since become a valuable asset in the analysis of the structure, organization and function of this chromosome (discussed below) (DAWE and CANDE 1996; HIATT and DAWE 2003a; HIATT and DAWE 2003b).

Molecular-genetic analysis of the Ab10 chromosome

In an effort to further analyze meiotic drive in maize, mutants of meiotic drive were generated using Robertson's *Mutator* (*Mu*) (DAWE and CANDE 1996; HIATT and DAWE 2003a; HIATT and DAWE 2003b), a transposable element in known to cause a high level of mutation in maize. The first mutant of meiotic drive, S*md 1* (originally called *smd 1*) was obtained in this way. The phenotype of *Smd 1* is a reduction of both preferential segregation and meiotic drive (DAWE and CANDE 1996), supporting Rhoades'

claim that neocentromere activity is required for meiotic drive. *Smd 1* was mapped to the region of Ab10 distal to the breakpoint of Df-C (FIGURE 1.3) (DAWE and CANDE 1996), and was later determined to be a dominant mutation based upon the inability of Ab10 to complement the effects of the *Smd 1* mutation (HIATT et al. 2002).

Two other mutants of meiotic drive found in the *Mu* screen were a deficiency of Ab10 called Df-L (HIATT and DAWE 2003a), and a second, cytologically normal mutant of meiotic drive, *smd 3* (HIATT and DAWE 2003a). Df-L lacks the distal tip of euchromatin (FIGURE 1.3), (HIATT and DAWE 2003a). Both Df-L and *smd 3*, unlike *Smd 1*, are recessive mutations that abolish meiotic drive, yet do not appear to result in a decreases in neocentromere activity (HIATT and DAWE 2003a). Using the deficiency series of Ab10 generated by Rhoades and Dempsey, *smd 3* was mapped to the region of Ab10 distal to the Df-K breakpoint and proximal to the Df-L breakpoint (FIGURE 1.3) (HIATT and DAWE 2003a).

Interestingly, most of the *Mu*-generated mutants of meiotic drive were the result of broken or rearranged Ab10 chromosomes rather than cytologically normal "point" mutations like *Smd 1* and *smd 3*. A total of five deletions and one duplicated Ab10 chromosome deficient in meiotic drive were recovered from the screen (HIATT and DAWE 2003a; HIATT and DAWE 2003b). This is an unusually high level of chromosome breakage (HIATT and DAWE 2003a; ROBERTSON et al. 1994), suggesting that Ab10 is unusually tolerant of breakage (HIATT and DAWE 2003a). Even the most severe deficiency uncovered, Df-B (FIGURE 1.3) was transmitted, although poorly, through the female gamete, indicating that the distal region of Ab10, comprising roughly 1.5% of the genome, is not essential for plant growth (HIATT and DAWE 2003b; RHOADES and

DEMPSEY 1985). The distal region of Ab10 may be viewed as a supernumerary element since it may be present or absent in different individuals and is therefore unnecessary for proper function of the organism (CARLSON 1977). Ab10 may have lost much of its originally essential genetic information and is under selection for its supernumerary, nonessential, function, in this case meiotic drive (OSTERGREN 1945).

Maize knobs are densely staining, heterochromatic regions of chromatin known to be composed primarily of two different tandemly repeated satellite sequences: the 180bp knob repeat and the 350bp TR-1 repeat (ANANIEV et al. 1998b; ANANIEV et al. 1998c; DENNIS and PEACOCK 1984; PEACOCK et al. 1981), as well as varying degrees of different retroelement families (ANANIEV et al. 1998b; MEYERS et al. 2001; MROCZEK and DAWE 2003) (discussed further in Chapter 3). Using the 180bp knob repeat to label knobs via in situ hybridization it was shown that neocentromeres, like native centromeres, interact with microtubule fibers of the spindle apparatus as they move toward the spindle poles during anaphase. However, neocentromeres interact with these fibers in a tangential manner, while ectopic centromeres appear to attach to microtubules in an end-on fashion (YU et al. 1997). The kinetochore is a large complex of proteins that attaches to the centromere during meiosis and is required for proper chromosome segregation. It has been shown that two of the major proteins of the kinetochore, CENP-C and MAD2, are absent from neocentromeres (DAWE et al. 1999). Additionally, maize neocentromeres do not associate with the centromeric histone H3 protein of maize, CENH3 (Dawe, unpublished data), a protein known to associate with all native maize centromeres. These results provided the first evidence that although neocentromeres appear to function in a

manner similar to that of proper centromeres, the molecular mechanisms underlying these two processes are different.

The deficient Ab10 chromosomes have also been utilized to better locate the factors necessary for the neocentromere activity of the chromosome (HIATT et al. 2002). Using both the 180bp and TR-1 knob repeats as in situ hybridization probes, it was shown that the large knob of Ab10 is comprised primarily of the 180bp repeat, while the three small chromomeres of the differential segment of Ab10 contain only the TR-1 knob repeat. Other knobs were shown to contain both the 180bp and TR-1 knob repeats (HIATT et al. 2002). Hiatt (2002) analyzed each of the Ab10 deficiencies for neocentromere activity, and discovered the presence of two different factors located on Ab10 that control neocentromere formation. One factor directs neocentromere activity of the 180bp repeat and is located distal to the Df-K breakpoint (FIGURE 1.3), and the second factor directs formation of neocentromeres at the TR-1 repeats of knobs and is located proximal to the breakpoint of Df-I (FIGURE 1.3) (HIATT et al. 2002). These findings explain the results of Emmerling (1959) who found that two of his most severe deficiencies, $Knob^0$ and $Knob^s$, still retained the ability to form neocentromeres at some knobbed monads during meiosis (EMMERLING 1959). Emmerling' s results are most likely explained by the retention of TR-1-mediated neocentromere activity by these deficiency chromosomes.

Meiotic Drive Systems of Other Organisms

Surprisingly, there are a number of meiotic drive systems present in nature and many share similar chromosomal organizations (Lyttle, 1991). Many drive systems

involve the selective dysfunction of a sensitive sex chromosome, or gametes containing the sensitive sex chromosome. The Ab10 chromosome, however, represents a case of autosomal chromosome drive. *Drosophila melanogaster* harbors an autosomal chromosome drive system called segregation distorter (SD), and several species of *Mus* (mouse) contain an autosomal segregation distortion system known as the t-haplotype.

In the SD system of *Drosophila*, males heterozygous for the SD locus produce 95-99% SD containing sperm, rather than the expected 50% SD and 50% SD^+ containing sperm. Females meiosis, however, appears to occur normally (LYTTLE 1991). The SD chromosome contains the drive locus (SD), an insensitive responder locus (Rsp^i), and can contain a number of enhancer loci. The sensitive chromosome (SD^+) contains a sensitive responder locus (Rsp^s) composed primarily of a 120-bp satellite repeat that is linked to the centromere (KUSANO et al. 2003; LYTTLE 1991) (see FIGURE 2.1A). The degree of sensitivity associated with a given SD^+ chromosome is directly related to the number of satellite repeats present at the Rsp^s locus (HOUTCHENS and LYTTLE 2003; LYTTLE 1991). SD^+ chromosomes also lack the enhancer loci. The strongest SD enhancer loci of the SD chromosome, as well as the Rsp^i locus of the SD chromosome are located in inverted regions, and the SD locus itself is within one map unit of this inversion (LYTTLE 1991) (see FIGURE 2.1A). These inversions significantly reduce the amount of recombination between the two chromosomes. Because of this, the SD and enhancer loci are prevented from recombining onto the chromosome containing the Rsp^s locus, the occurrence of which would essentially eliminate the drive system (LYTTLE 1991).

Much of the molecular mechanism of the SD system has been deciphered. The SD locus is a dominant gain of function mutation that produces a truncated Ran-GAP protein

(KUSANO et al. 2003; MERRILL et al. 1999). Normally this protein is located in the cytosol and acts as part of the Ran signaling pathway involved in nuclear localization of proteins (KUSANO et al. 2003). Truncation of the protein produced by SD causes mislocalization of the protein into the nucleus, and ultimately results in the improper condensation of the satellite DNA of the Rsp^s locus (KUSANO et al. 2003; MERRILL et al. 1999). The insensitivity of the SD chromosome is though to be due to the fact that the Rsp^i locus contains less than 20 copies of the 120-bp repeat (LYTTLE 1991).

In the t-haplotype segregation distortion system of *Mus*, males that are heterozygous for the drive chromosome (t/+) can produce up to 99% t-haplotype containing sperm. Females however, as in the SD system of *Drosophila*, produce normal gametic ratios (HAMMER et al. 1991; LYTTLE 1991). The t-haplotype drive system is the result of four distorter loci and a responder locus located in four separate inversions on chromosome 17 (HAMMER et al. 1991; LYTTLE 1991) (see FIGURE 2.1B). Again, like in the SD system, these inversions serve to maintain the distorter and responder loci of the drive chromosome in a genetic complex (this genomic region is referred to as the t-complex) that is unable to recombine with its wild-type homologue.

Although the exact mechanism of t-haplotype mediated sperm dysfunction is unknown, some of the components have been revealed. Each distorter locus examined so far produces a mutant protein involved in spermatid function. One distorter protein is an axonemal dynein heavy chain involved in flagellar development (SAMANT et al. 2002). Another distorter protein is a dynein light chain, also implicated in flagellar organization (PATEL-KING et al. 1997), and two other proteins encoded by the t-complex are involved in sperm-oocyte interaction and fusion (REDKAR et al. 2000). Although the responder

locus of the system is unknown, it has been postulated that the distorter proteins produced by the t-complex act as dominant mutations. The model is that spermatids containing the t-complex responder locus are somehow able to eliminate or avoid accumulating the mutant proteins. Spermatids containing the wild-type responder locus accumulate these defective proteins and are rendered dysfunctional (PATEL-KING et al. 1997). In both the SD and t-haplotype systems a key element of segregation distortion is that the genes are organized on the chromosome such that they are unable to recombine with their sensitive homologous chromosomes.

Centromere Structure

In all chromosomes the centromere is the location of kinetochore formation and microtubule attachment during mitosis and meiosis. Although centromere function remains constant across all life forms, the underlying DNA sequence is highly variable even among closely related species (CHOO 2001; HENIKOFF et al. 2001; HESLOP-HARRISON et al. 2003). Although there is no sequence similarity among centromeres of divergent species, a universal property of centromeric DNA appears to be its association with a centromeric histone H3 protein (CENH3). Association of the DNA with these histones results in the formation of centromeric nucleosomes at which the kinetochore assembles and attaches to the spindle fibers (CHOO 2001; HENIKOFF et al. 2001; SUN et al. 1997). Another similarity among nearly all centromeres examined is the presence of tandemly-repeated satellite sequences and other repetitive DNA sequences like transposable elements (AMOR and CHOO 2002; ANANIEV et al. 1998a; CHENG et al. 2002; CHOO 2001; HENIKOFF et al. 2001; HESLOP-HARRISON et al. 2003; KUMEKAWA et al.

2001; NAGAKI et al. 2003b; SUN et al. 1997). The tandem repeat arrays found in many plant and animal centromeres are centromere-specific (AMOR and CHOO 2002; ANANIEV et al. 1998a; CHENG et al. 2002; CHOO 2001; HUDAKOVA et al. 2001; KUMEKAWA et al. 2000; KUMEKAWA et al. 2001; ZHONG et al. 2002). Additionally, the lengths of these individual centromere repeats are quite similar (between 150-200bp) across a wide range of organisms (HENIKOFF et al. 2001).

Maize centromeres are composed of long tracts of a 156-bp tandemly repeated satellite sequence called CentC (ANANIEV et al. 1998a). These repeats are interrupted by members of the retroelement families CentA (ANANIEV et al. 1998a) and CRM (ZHONG et al. 2002) (FIGURE 1.4A). Although over 50% of the maize genome is composed of retroelements (BENNETZEN et al. 1998; SANMIGUEL and BENNETZEN 1998; SANMIGUEL et al. 1996), neither CentA nor CRM are found at regions of the genome other than the centromeres (ANANIEV et al. 1998a; ZHONG et al. 2002). The Cent C satellite and both of the retroelements have been shown to interact with the maize centromeric histone H3, CENH3, by chromatin immunoprecipitation (ZHONG et al. 2002). These results indicate that both the satellite sequence and the retroelements have potential functions in formation of the kinetochore complex. The *Arabidopsis* CENH3 protein, HTR12, also interacts primarily with a centromere-specific 180-bp satellite repeat (NAGAKI et al. 2003b). The tandem repeats are interrupted by a variety of retroelement sequences, but unlike in maize, these retroelements do not interact with CENH3 (FIGURE 1.4B) (BRANDES et al. 1997; INITIATIVE 2000; KUMEKAWA et al. 2000; KUMEKAWA et al. 2001; NAGAKI et al. 2003b).

In contrast to these observations, the centromeres of *Drosophila* are composed primarily of a satellite repeat that is only 5-bp in length interspersed with a few transposable elements (CHOO 2001; SUN et al. 2003; SUN et al. 1997). Neither the satellite repeats nor the transposable elements are centromere specific (CHOO 2001; SUN et al. 2003; SUN et al. 1997). Additionally, these sequences are not found at every *Drosophila* centromere (SUN et al. 1997). Despite the differences in satellite DNA composition, the *Drosophila* homologue of CENH3, Cid, is found at all *Drosophila* centromeres (CHOO 2001; MALIK and HENIKOFF 2001).

Human centromeres and neocentromeres present yet another story (FIGURE 1.4C and D). All native autosomal centromeres in humans contain an ~171-bp satellite repeat called the α-satellite that binds the human CENH3, CENP-A (AMOR and CHOO 2002; CHOO 2001). Human neocentromeres, however, all bind CENP-A, but lack the α-satellite sequence (AMOR and CHOO 2002; CHOO 2001). These neocentromeres arise at a variety of locations on broken chromosomes that have lost the native, α-satellite containing, centromere. Unlike the human neocentromeres, the neocentromeres of maize do not interact with maize CENH3 (Dawe, unpublished data). Maize neocentromeres also lack the kinetochore proteins CENP-C and MAD2 (DAWE et al. 1999), and the satellite repeats of maize knobs do not co-precipitate with CENH3 in ChIP experiments (ZHONG et al. 2002). These results indicate that maize neocentromeres do not associate with kinetochore nor do they function in the same manner as native centromeres. How, exactly, maize neocentromeres accomplish poleward movement along microtubules during cell division is presently unknown.

The fact that centromeric DNA sequences vary widely but they interact with CENH3 proteins (CHOO 2001; HENIKOFF et al. 2001), suggests that the primary DNA sequence of centromeres is relatively insignificant. The significance of centromeric DNA sequences probably comes from a specialized organization of the DNA sequences into an overall structure that retains an association with CENH3.

Purpose of this Study

The overall intent of this study is to better understand the structure, organization, and composition of the Abnormal 10 chromosome of maize. The following chapters and appendix detail the efforts undertaken to analyze the physical structure and organization of this chromosome as well as its relative composition of transposable elements.

As discussed above, the physical structure of a meiotic drive system is critical to its origin and maintenance of the system (LYTTLE 1991). Chapter 2 details the efforts taken to elucidate the physical structure of Ab10. Both classical genetic mapping techniques and molecular mapping methodologies were used to create an integrated map of the N10 chromosome. A molecular map of the Ab10 chromosome was created using the available deficiency chromosomes of Ab10 and compared to the newly integrated N10 map in order to define the borders of the Ab10 inversion molecularly.

In Chapter 3, I present an analysis of the distribution of retroelements with respect to the Ab10 chromosome as well as the rest of the maize genome, particularly with respect to the satellite repeats of the maize centromeres and knobs. Using fluorescent in situ hybridization (FISH), I was able to define particular accumulation patterns of

retroelement families with respect to the satellite sequences examined, as well as the Ab10 chromosome.

As mentioned earlier, a factor or factors necessary for Ab10 mediated meiotic drive exists in the distal tip of euchromatin located on Ab10 (HIATT and DAWE 2003a). Early analysis of the distribution of miniature inverted-repeat transposable elements (MITEs) in maize found that they were often associated with genes (ZHANG et al. 2000). In the Appendix, I review transposon display experiments undertaken in an attempt to uncover MITEs located on Df-L, and potentially in a gene(s) required for meiotic drive. Although a gene necessary for meiotic drive was not found using this method, I present data on the accumulation of MITEs with respect to the distal tip of the Ab10 chromosome.

FIGURE 1.1: The maize karyotype. Karyotype of maize containing the Ab10 chromosome showing the 10 chromosomes of maize and the Ab10 chromosome. The chromomeres, inverted region, large knob and distal tip of Ab10 are labeled. Centromeres for each chromosome are indicated with a green dot. Knobs are indicated by red arrows.

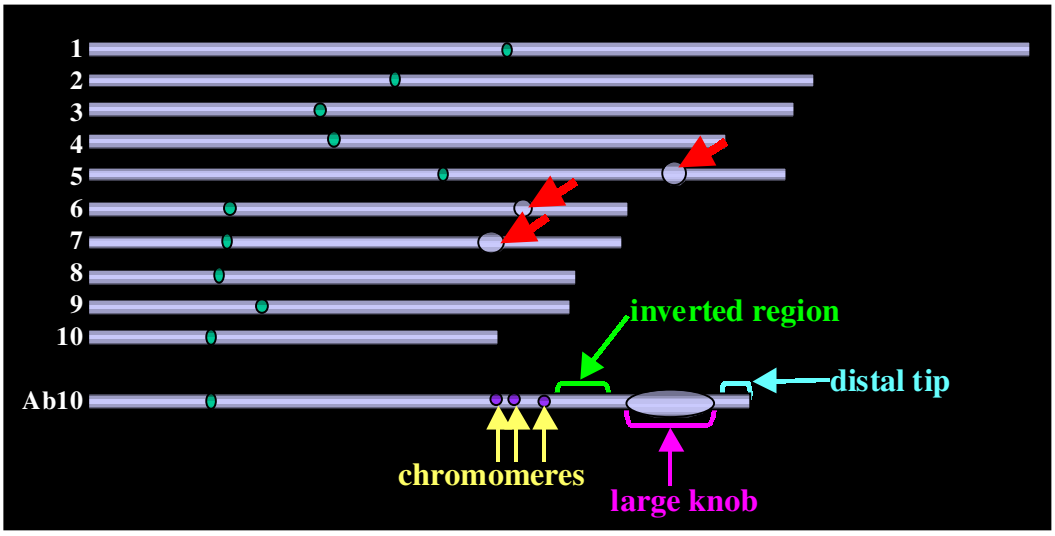
1
2
3
4
5
6
7
8
9
10
Ab10
inverted region
distal tip
chromomeres
large knob

FIGURE 1.2: Rhoades' model for meiotic drive in maize. A single pair of homologous chromosomes, heterozygous for the presence of a knob, are diagrammed through female meiosis in maize. In step 1, replication of the chromosomes and crossing over between the knob and centromere occurs. In step 2, neocentromere activity during meiosis I pulls the knobbed chromatid of the heteromorphic dyad to the poles ahead of the ectopic centromere. In step 3, the factor(s) necessary for meiotic drive maintain the peripheral position of the knobs so that they are pulled into the two terminal cells during meiosis II. Because only the basal cell of the tetrad continues development into an egg, the terminal location of the knobs results in their preferential segregation.

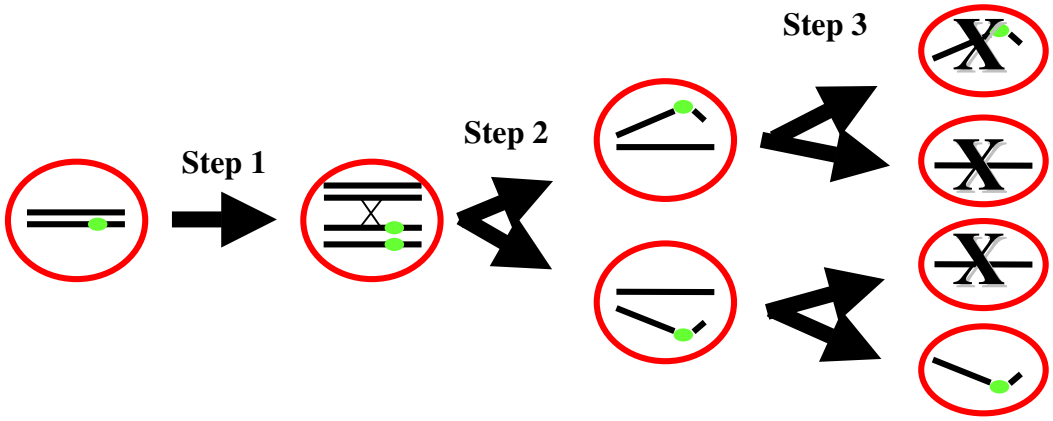
Step 1
Step 2
Step 3

FIGURE 1.3: Deficiencies of the Ab10 chromosome. Diagrams of N10 and the Ab10 chromosomes showing the breakpoint location for each of the deficiencies. K^0 and K^S were discovered by Emmerling (1959). KV was discovered by Miles (1970). Df-C, Df-I, Df-F, Df-H, and Df-K were discovered by Rhoades and Dempsey (1985). Df-L and Df-B were discovered by Hiatt et al. (2003). The name of the deficiency is given to the left of each line showing the location of its breakpoint. The approximate locations for the functions associated with Ab10 are indicated with red bars below the diagram.

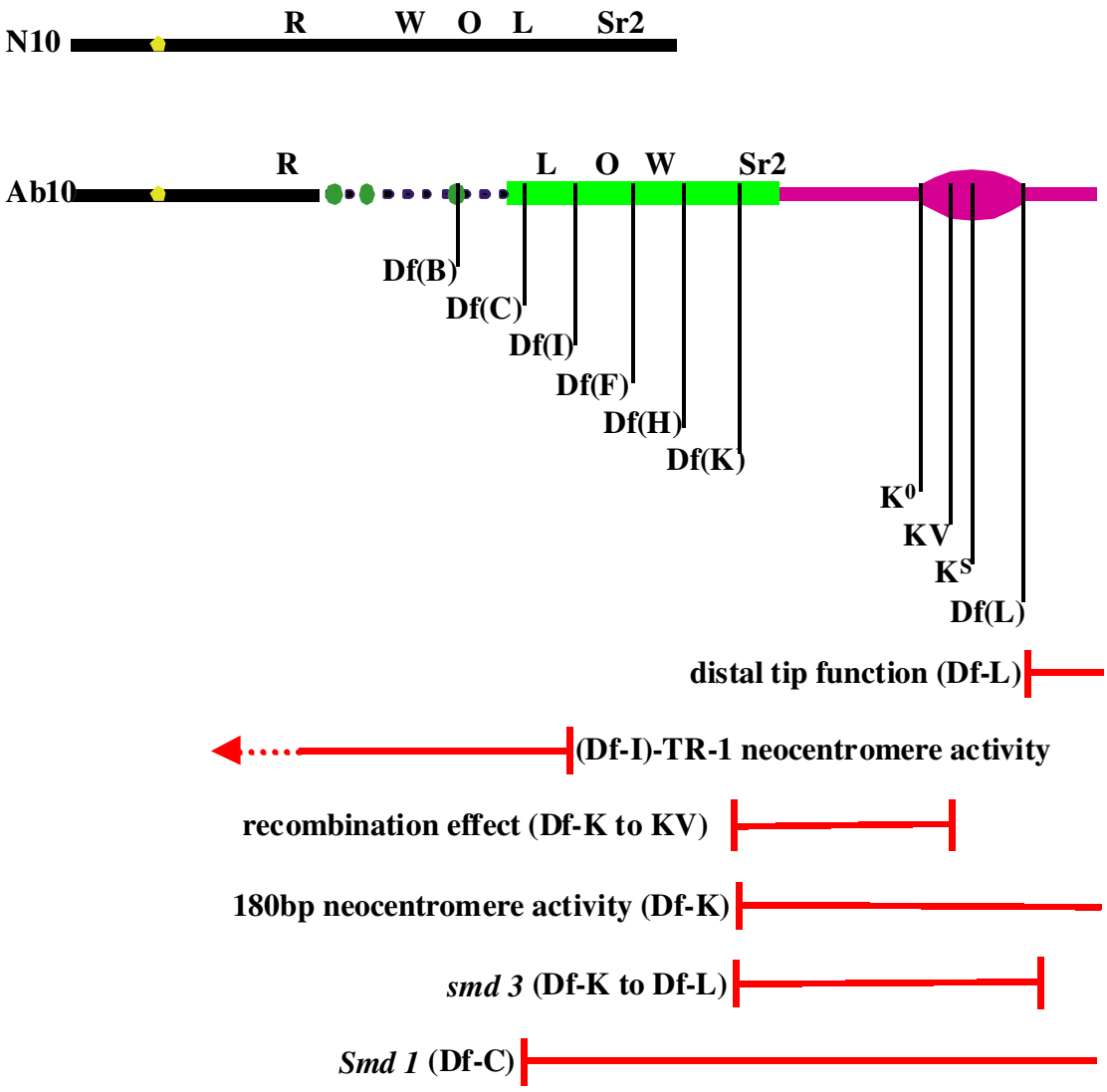
N10
R
W
O
L
Sr2
Ab10
R
L
O
W
Sr2
Df(B)
Df(C)
Df(I)
Df(F)
Df(H)
Df(K)
K0
KV
KS
Df(L)
distal tip function (Df-L)
(Df-I)-TR-1 neocentromere activity
recombination effect (Df-K to KV)
180bp neocentromere activity (Df-K)
smd 3 (Df-K to Df-L)
Smd 1 (Df-C)

FIGURE 1.4: Representative centromere structures. A. Diagram of a maize centromere. Centromeric DNA is shown in pink, pericentromeric heterochromatin in red. CentC, CentA and CRM bind to CENH3. B. Diagram of an *Arabidopsis* centromere. Centromeric DNA that attaches to HTR12 is shown in light purple, pericentromeric heterochromatin is shown in dark purple. Centromeric region is blown up to show the relative composition of the centromere: predominantly tandemly repeated 180-bp satellite sequence interspersed with DNA elements and retroelements. The retroelement sequences, however, do not interact with HTR12. C. Diagram of a human centromere. Centromeric DNA bound by CENP-A is shown in light blue, pericentromeric heterochromatin is shown in dark blue. Human centromeres are composed predominantly of tandem copies of the α-satellite repeat with increasing numbers of transposable elements near the ends of the centromere. D. Diagram of a human neocentromere lacking the α-satellite. CENP-A binds to non α-satellite DNA sequences in human neocentromeres.

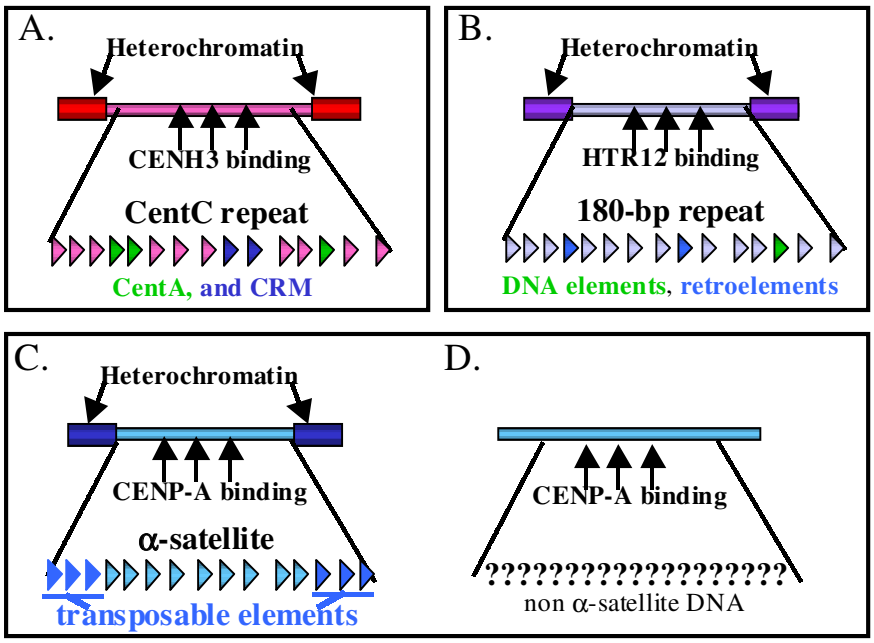
A.
Heterochromatin
CENH3 binding
CentC repeat
CentA, and CRM
B.
Heterochromatin
HTR12 binding
180-bp repeat
DNA elements, retroelements
C.
Heterochromatin
CENP-A binding
α-satellite
transposable elements
D.
CENP-A binding
??????????????????
non α-satellite DNA

CHAPTER 2

MULTIPLE CHROMOSOMAL REARRANGEMENTS OCCURRED DURING THE EVOLUTION OF THE MAIZE MEIOTIC DRIVE SYSTEM[1]

[1] Mroczek, R.J., J.R. Melo and R.K. Dawe. 2003. To be submitted to *Genetics*.

Introduction

Meiotic drive describes a variety of phenomena that causes the preferential segregation of alleles or haplotypes to the next generation. Many meiotic drive systems involve the preferential segregation of a particular sex chromosome. In *Drosophila*, several African butterfly species, and the wood lemming *Myopus schisticolor*, there are meiotic drive systems that cause an excess of female progeny. In two mosquito species, *Aedes aegypti* and *Culex quinquefasciatus*, male-chromosome drive systems have been described (LYTTLE 1991). Some of the best studied meiotic drive systems, however, such as the *t*-haplotype of mouse, *Segregation Distorter* in *Drosophila*, and Abnormal chromosome 10 of maize, cause autosomal meiotic drive (LYTTLE 1991; RHOADES 1942).

Regardless of the type of meiotic drive, linkage disequilibrium among the components of the drive system is almost always observed (LYTTLE 1991; RHOADES and DEMPSEY 1985). A case in point is the segregation distorter (SD) system of *Drosophila*, which causes almost 99% of the sperm from males heterozygous for SD to carry the SD drive system. The SD locus is found in tight-linkage with a pericentric inversion that contains an insensitive responder (Rsp^{i}) locus as well one or more enhancer loci and often a second inversion (FIGURE 2.1A) (LYTTLE 1993). SD produces a truncated Ran-GAP protein that interferes with chromosome condensation in gametes containing the wild type form of the responder locus (Rsp^{s}) (KUSANO et al. 2003; LYTTLE 1991). Because of the sensitivity of Rsp^{s} to the SD protein product, recombination between SD and Rsp^{s} would produce a suicidal chromosome. The combination of tight linkage and inversions effectively prevents recombination and serves to preserve the SD meiotic drive system in *Drosophila*.

A similar situation exists in the *t*-haplotype system of mouse, where males heterozygous for the *t*-haplotype autosome produce nearly all *t*-haplotype containing sperm (LYTTLE 1991). The *t*-haplotype is contained on the telocentric chromosome 17, and contains four inverted regions spanning the proximal-most 18 centimorgans of the chromosome (FIGURE 2.1B) (HAMMER et al. 1991). Within this region are the responder locus and at least four drive loci (HAMMER et al. 1991; LYTTLE 1991). Like the SD system of *Drosophila*, the complex of inversions prevents recombination between the drive and non-drive chromosomes such that the integrity of the *t*-haplotype is maintained throughout successive meiotic cycles.

The Abnormal 10 chromosome (Ab10) of maize causes the preferential segregation of condensed heterochromatic regions called knobs to the next generation (RHOADES 1942). Ab10 is cytologically distinguishable from N10 by a large segment of additional chromatin attached to the long arm of the chromosome. The additional chromatin is comprised of a 'differential segment' which contains three small chromomeres, a euchromatic region that contains an inverted portion of the N10 chromosome, a large heterochromatic knob, and a small euchromatic distal tip (RHOADES 1942; RHOADES and DEMPSEY 1985). Maize knobs, the responding loci of the Ab10 mediated drive system, are composed of one or a combination of two satellite repeat sequences; the 180bp-knob repeat and the 350-bp TR-1 knob repeat (ANANIEV et al. 1998b; ANANIEV et al. 1998c; DENNIS and PEACOCK 1984; HIATT et al. 2002).

Knobs experience meiotic drive because they are preferentially segregated to the basal-most cell of the linear tetrad during female meiosis. The basal megaspore is the only daughter cell that produces an egg in maize and some other angiosperms (the upper

three cells degenerate and die). The Ab10 chromosome produces four functions that ensure the placement of knobbed chromatids in the basal cell, and these functions have been mapped on Ab10 using terminal deficiencies (HIATT and DAWE 2003a; RHOADES 1942) (FIGURE 2.2). Several of these functions are known, and can be ordered with respect to a model for meiotic drive put forward by Rhoades (1942). First, Ab10 results in an increase in the amount of recombination between knobbed and non-knobbed chromosomes, producing heteromorphic dyads at the onset of meiosis (KIKUDOME 1959; RHOADES and DEMPSEY 1966). The recombination effect has been mapped to a region of Ab10 between the breakpoint of deficiency-K (Df-K) and the first third of the large knob (HIATT and DAWE 2003a; MILES 1970). Next, Ab10 results in the transformation of knobs into neocentromeres that move ahead of the native centromeres during anaphase (RHOADES 1942). Neocentromere activity is provided by two separate functions on Ab10; one mobilizes 180-bp repeats and maps distal to the Df-K breakpoint and the second mobilizes TR-1 repeats and maps proximal to the deficiency-I (Df-I) breakpoint (FIGURE 2.2) (HIATT et al. 2002). The peripheral location of the knobbed dyads is preserved throughout interkinesis, such that knobbed chromatids are in the outer-most cells following meiosis II (RHOADES 1942). The final step(s) may be carried out by a factor known as the distal tip function or by either of two characterized mutations of meiotic drive, *Smd1* and *smd3* (FIGURE 2.2) (DAWE and CANDE 1996; HIATT and DAWE 2003a).

The single known inversion on Ab10 (FIGURE 2.2) was identified using the same series of deficiencies used to map the various functions associated with meiotic drive (RHOADES and DEMPSEY 1985). The inversion spans a region containing the *W2, O7,*

and *L13* loci such that the order of genes on Ab10 is *L13, O7, W2*. In an effort to better understand the nature of this rearrangement, we integrated the molecular and genetic maps of normal chromosome 10 and mapped 12 RFLP markers onto Ab10. We find that the known inversion on Ab10 is actually a more complex rearrangement comprised of at least two separate inversions.

Materials and Methods

Integration of *Sr2* with the molecular map

Homozygous *R-Isr*/*R-Isr*, *Sr2*/*Sr2* seeds in the B73 background and homozygous *r-isr*/*r-isr*, *sr2*/*sr2* seeds, probably in the W22 background, were obtained from the Maize Genetics Cooperation Stock Center (Urbana, IL). Seeds were germinated in the greenhouse and plants were crossed to create the F1 generation. The F1 plants were selfed to generate a segregating F2 population. One hundred *r-isr*/*r-isr* F2 seeds were germinated and plants were screened for *sr2*/*sr2* homozygotes. Only *r-isr*/*r-isr* seeds were planted because the *Isr* locus, tightly linked to *R*, inhibits the *sr2*/*sr2* phenotype.

Tissue was collected from 32 striped (*sr2*/*sr2*) plants and 50 green (*Sr2*/*Sr2* or *Sr2*/*sr2*) plants. DNA was isolated from each F2 individual, as well as from the original parents of the F1. DNA from both parents and each of the progeny was digested with *Bgl*II and prepared for Southern blot hybridization. Southern blotting was performed using ^{32}P-labeled RFLP probes. Hybridization was carried out at 45°C in a 50% formamide buffer containing 1M NaCl, 2% SDS, 10% dextran sulfate and 0.1 mg/mL denatured salmon sperm DNA. RFLP probes were PCR amplified from plasmids obtained from the Maize Mapping Project (Columbia, Missouri). Linkage analysis of the

RFLP markers as well as the *R* and *Sr2* genes was performed using Mapmaker Version 3.0 (LANDER et al. 1987) using a LOD score of 3.0 and a recombination fraction of 35 Kosambi centimorgans. This map was then aligned with the genetic map of the region as well as three other RFLP maps of the chromosome (UMC 1998, BNL 2002, and IBM neighbors 10; http://www.maizegdb.org/map.php) using GenomePixelizer (Release May 05 2003) (KOZIK et al. 2002). *R*, *Sr2* and all of the RFLPs used in the Ab10 analysis were placed onto a compilation map and used for comparison to Ab10.

RFLP Mapping of Ab10

The Ab10 and Ab10 deficiencies C, I, F, H, and K were originally described by Rhoades and Dempsey (1985), and deficiency L was described by Hiatt and Dawe (2003). Ab10 and all deficiencies were backcrossed into the W23 background at least 5 times and maintained in the heterozygous condition.

DNA was isolated from each genotype. For preliminary screening, DNA from N10, Ab10/N10 and Df-C/N10 were analyzed for polymorphisms using six different restriction enzymes, and Southern blotted for ^{32}P-labeled RFLP analysis. A total of 22 RFLP markers were analyzed. Those polymorphic RFLPs absent on Df-C were then assayed on the entire deficiency series. The following probes were examined and showed no polymorphism between N10 and Ab10: csu300b, uaz294, asg50d, csu1039, bnl7.02, csu844, asg81, csu615, isu53, and asg19.

Results

Integration of the *Sr2* locus into the N10 RFLP map

Of the genes known to exist on the distal portion of chromosome 10, only the *R* locus has been mapped onto the RFLP maps. In order to perform an RFLP analysis of the Ab10 chromosome using the Rhoades and Dempsey deficiencies (FIGURE 2.2), we first needed to integrate the *Sr2* locus onto the RFLP map of N10. The *Sr2* locus is the most distal locus on the N10 genetic map and is also distal to the previously-described inversion on Ab10 (FIGURE 2.2) (RHOADES and DEMPSEY 1985). By creating an RFLP map containing both the *R* and *Sr2* loci, the relative order of RFLPs spanning the entire known inverted region could be determined.

In order to integrate the *Sr2* locus onto the RFLP map a mapping population was created by crossing homozygous recessive r/r, *sr2*/*sr2* plants (yellow kernel, striped plants), to homozygous dominant *R*/*R*, *Sr2*/*Sr2* plants (red kernel, green plant). F1s were selfed to create a segregating F2 population. Tightly linked to the *R*-locus is another locus called inhibitor of striate (*Isr*) that prevents the *sr2* phenotype from being expressed (KERMICLE and AXTELL 1981; PARK et al. 2000). Because of this only the homozygous *r-isr*/*r-isr* kernels that allow for *striate leaves* expression were used for segregation and mapping analysis.

F2 kernels were planted and screened for the striate leaves phenotype after emergence of the fifth leaf. Tissue was collected from all striped or green plants for a total of 82 plants. DNA was prepared from these progeny as well as from the two original parents of the cross and scored for two single-copy RFLP markers, gln1, and csu48. Csu48 is one of the most distally located RFLPs on the N10 chromosome and was used to ensure coverage of N10 through end of the molecular map. Mapmaker was used to place the four markers in the following order (proximal to distal): *R*-29.9cM-gln1-

8.6cM-csu48-6.9cM-*Sr2*, Our map places the *Sr2* locus as the distal most marker on both the genetic and RFLP maps of the N10 chromosome (FIGURE 2.3).

Once *Sr2* was integrated onto the RFLP map, we used the GenomePixelizer program (KOZIK et al. 2002), to compare our map with the genetic map of N10 and three molecular maps of the chromosome: UMC1998, BNL2002, and IBM neighbors. The five maps were then aligned by hand and used to generate a ' consensus' map of the N10 chromosome between the *R* and *Sr2* loci (FIGURE 2.3). This map includes only those RFLPs that were analyzed on the Ab10 chromosome and lists them in their relative order to each other. No cM distances can be assigned using this approach because each map was derived from a different mapping population.

Molecular mapping of the inversion on the Ab10 chromosome

A molecular map of the Ab10 chromosome was created using the terminal deficiencies Df-C, Df-I, Df-F, Df-H, Df-K and Df-L. A collection of maize RFLP markers located distal to the *R* locus on the long arm of N10 were first analyzed for polymorphism between N10 and Ab10 and for the presence or absence of this polymorphic marker on the Df-C chromosome. Six different restriction *enzymes (EcoRI, BglII, BamHI, HindIII, SacI,* and *XbaI*) were used to analyze each of the genotypes. Southern hybridization was used to identify RFLP markers present in the Ab10 genotype but missing in both the N10 and Df-C genotypes. These markers are located in the region of Ab10 distal to the Df-C breakpoint, where the known inversion lies. Those markers polymorphic on Ab10 but present in Df-C are likely to be located somewhere in the region between *R* and the Df-C breakpoint (see FIGURE 2.2), a region containing the

differential segment and some euchromatic DNA. Of the 22 RFLP markers examined, five markers were found to be located proximal to the Df-C breakpoint (FIGURE 2.4A) and seven located distal to the Df-C breakpoint. For the other 10 RFLP markers, no polymorphisms were detected. An absence of polymorphism could mean either that the marker is proximal to *R* and the N10 allele was recombined onto Ab10 during backcrossing, or that the N10 and Ab10 alleles are so similar that they cannot be distinguished using six restriction enzymes.

The map positions of the seven RFLP loci located distal to the Df-C breakpoint were further refined using the full deficiency series of Ab10. DNA from each of the deficiency genotypes along with N10 and Ab10 was digested with an enzyme that resulted in polymorphisms in the preliminary analysis. These genotypes were then analyzed by Southern hybridization using the distally located RFLP probes. Each of these RFLP markers is expected to be absent in Df-C but to re-appear in one of the less severe deficiencies (FIGURE 2.4B). For example, the csu48 RFLP reveals a polymorphic band that is missing in Df-C and Df-I, yet is present in deficiencies F, H, K and L. This places csu48 between the Df-I and Df-F breakpoints of Ab10. The same methodology was used to map the other six RFLP markers that were distal to the Df-C breakpoint. The resulting RFLP map of Ab10 is shown in Figure 2.5.

Comparison of the newly created N10 and Ab10 molecular maps (FIGURE 2.5) revealed the presence of a more complex chromosomal rearrangement than was originally described. Of the seven distally located markers on Ab10, npi421b was found to have the most distal location on Ab10, between the breakpoints of Df-F and Df-H. On the N10 map however, this marker is located proximal to the other six markers.

Additionally, five RFLP markers located just proximal to npi421b on the N10 map (npi290, bnl7.49, uaz251, npi306, and isu163) all map proximal to the Df-C breakpoint. This indicates that npi421b marks the proximal end of an inversion. If this were a simple inversion, one would expect that the most distal markers on N10, csu48 and dba3, would occupy the most proximal locations on Ab10. However, csu48 and dba3 are both located between the breakpoints of Df-I and Df-F, in the middle of the expected inversion. Conversely, the csu571 and csu781 markers, located between gln1/umc232 and csu48/dba3 on the N10 map, are located proximally to both markers on the Ab10 molecular map. Taken together these data indicate that the chromosomal rearrangements between N10 and Ab10 represent at least two separate inversions.

Discussion

Chromosomal rearrangements that reduce or eliminate recombination have been found in nearly every well characterized meiotic drive system (HAMMER et al. 1991; LYTTLE 1991; PATEL-KING et al. 1997). Generation of linkage disequilibrium among the drive and responder loci ensures that components of the drive system are not lost or transferred onto the susceptible chromosome, where they might produce "suicidal" chromosomes. Linkage disequilibrium, therefore, becomes a necessity for both the origin and maintenance of meiotic drive systems (LYTTLE 1991). An inversion within the meiotic drive system on Ab10 was previously discovered and analyzed in relation to the genes located in the region (RHOADES and DEMPSEY 1985). Here we have used RFLP mapping to show that the inversion identified by Rhoades and Dempsey is actually composed of two inversions.

Previous analyses had placed *Sr2* close to the large knob of Ab10 and near the distal end of the inversion. In order to molecularly map the Ab10 chromosome we first integrated the *Sr2* locus onto the N10 RFLP map and created a compilation map of markers located between these two genes on N10 (FIGURE 2.3). A RFLP map of Ab10 was then created by taking advantage of a series of terminal deficiencies (FIGURE 2.5).

Comparison of the N10 RFLP map and the molecular map obtained for Ab10 reveals a complex rearrangement of RFLP markers on Ab10 that is most likely the result of a nested inversion. In Figure 2.6 we propose a possible model for how N10 was rearranged to create the organization of markers observed on Ab10. The data suggest a small inversion occurred involving the csu781a/csu571b loci and the csu48/dba3 loci. This small inversion placed csu48/dba3 distal to gln1/umc232 and proximal to csu571 and csu781 (since the csu571 and csu781 have been separated from each on the Ab10 map with csu781 being proximal to csu571, they have been separated from each other on the N10 map as well). Another larger inversion occurred beginning proximal to the npi421b locus and extending distally to include all RFLPs up to a location proximal to the *Sr2* locus. Although the model diagrams the small inversion occurring first, the two inversions could have arisen in either order.

As in other drive systems, we believe that the complex chromosomal rearrangements on Ab10 serve to maintain linkage among the drive components of the system. Recombination events that separated the neocentromere factors or the recombination effect from the distal tip function would not result in a suicidal chromosome, like in the SD system of *Drosophila*. Nevertheless, separation of the drive functions would result in ineffectively-driven Ab10 chromosomes that would be lost

from the population. Comparison of the RFLP map of Ab10 with its known functions (FIGURES 2.2 and 2.5) shows that the proximal breakpoints of both the large and small inversions extend into the region where the TR-1 repeat neocentromere function lies. The distal breakpoint of the large inversion lies in a region close to the 180-bp repeat neocentromere function. Even a single inversion in this region would effectively isolate the neocentromere-promoting factors from each other as well as from the wild type chromosome; but here we have two inversions. Data from *Drosophila* indicate that nested inversions are significantly more effective at preventing recombination than single inversions (BEADLE and STURTEVANT 1935). It appears that the terminal portion of Ab10 has experienced a degree of rearrangement that is sufficient to nearly eliminate recombination with N10.

Our observations are especially noteworthy in light of the fact that naturally occurring inversions are exceedingly rare in maize. A survey of 90 land races of maize revealed only one inversion (RHOADES and DEMPSEY 1953). To our knowledge, the nested inversion described here is the first complex inversion identified in this species. Taken together, these data strongly support the view that chromosome rearrangements are a key element in the evolution of successful meiotic drive systems.

FIGURE 2.1: Diagrammatic representation of the SD and t-haplotype chromosomes. In each chromosome the centromeres are shown in gray and the pericentromeric heterochromatin is shown as darker boxes than the surrounding DNA. A. The segregation distorter chromosome of *Drosophila* is shown on top, the wild-type homologue is shown below. The inverted regions of the SD chromosome are shown bounded by red parentheses. E signifies enhancer sequences of the SD system. B. The t-haplotype chromosome of *Mus* is shown on top, the wild-type homologue is shown below. The four inverted regions containing the drive loci are indicated by large boxes and are numbered 1-4. These figures were adapted from figures in Kusano et al. (2003), and Lyttle (1991).

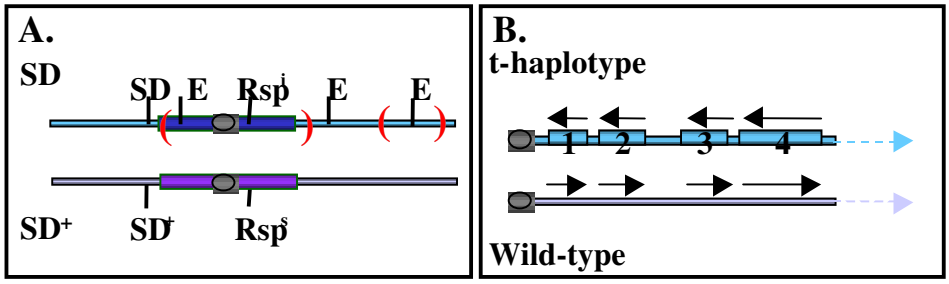
A.
SD
SD E Rsp^i E E
SD+ SD+ Rsp^s
B.
t-haplotype
1 2 3 4
Wild-type

FIGURE 2.2: Graphical representations of the N10 and Ab10 chromosomes. The breakpoints of each of the deficiency chromosomes are indicated. The four functions provided by Ab10 have been mapped with respect to the deficiency series of the chromosome by Hiatt et al, 2003 and are indicated below the Ab10 diagram, as well as the location of the *smd 3* mutation. The differential segment is indicated by the dashed line and chromomeres are represented by green dots. The known inversion on Ab10 is indicated by a green box.

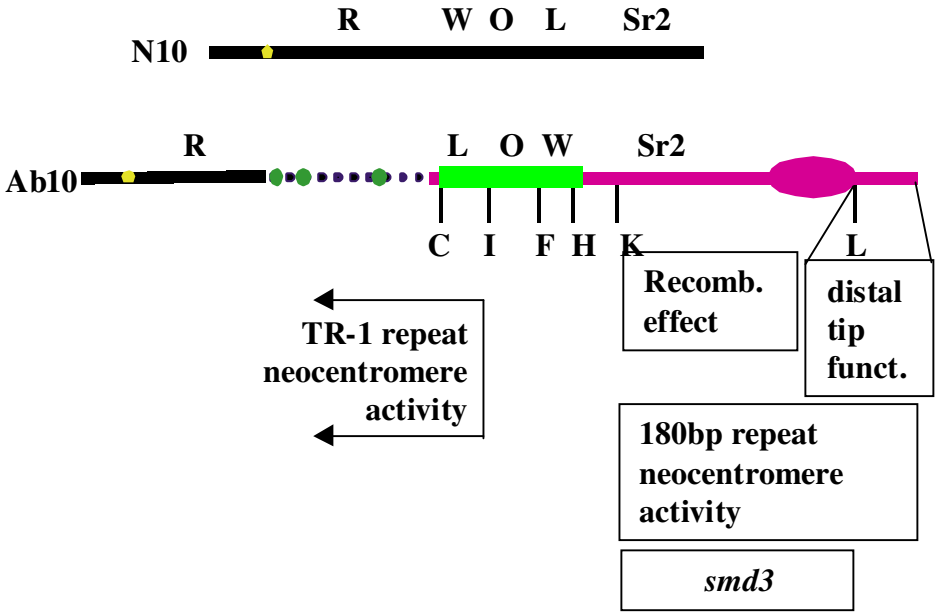
R
W O L
Sr2
N10
R
L O W
Sr2
Ab10
C I F H K
L
Recomb. effect
distal tip funct.
TR-1 repeat neocentromere activity
180bp repeat neocentromere activity
smd3

FIGURE 2.3: Molecular and genetic maps of N10. Five maps of the N10 chromosome maps and our consensus map are shown. The top five maps represent four published maps and the map created here, the names of each map are labeled. The *isu163* locus was added to the IBM neighbors map based upon its tight linkage to rz569a on the CU 99 10 map. The bottom map represents a consensus map created by linking each of the available maps of this region of N10. Only those RFLPs used in the Ab10 mapping analysis are labeled in order to simplify the final map.

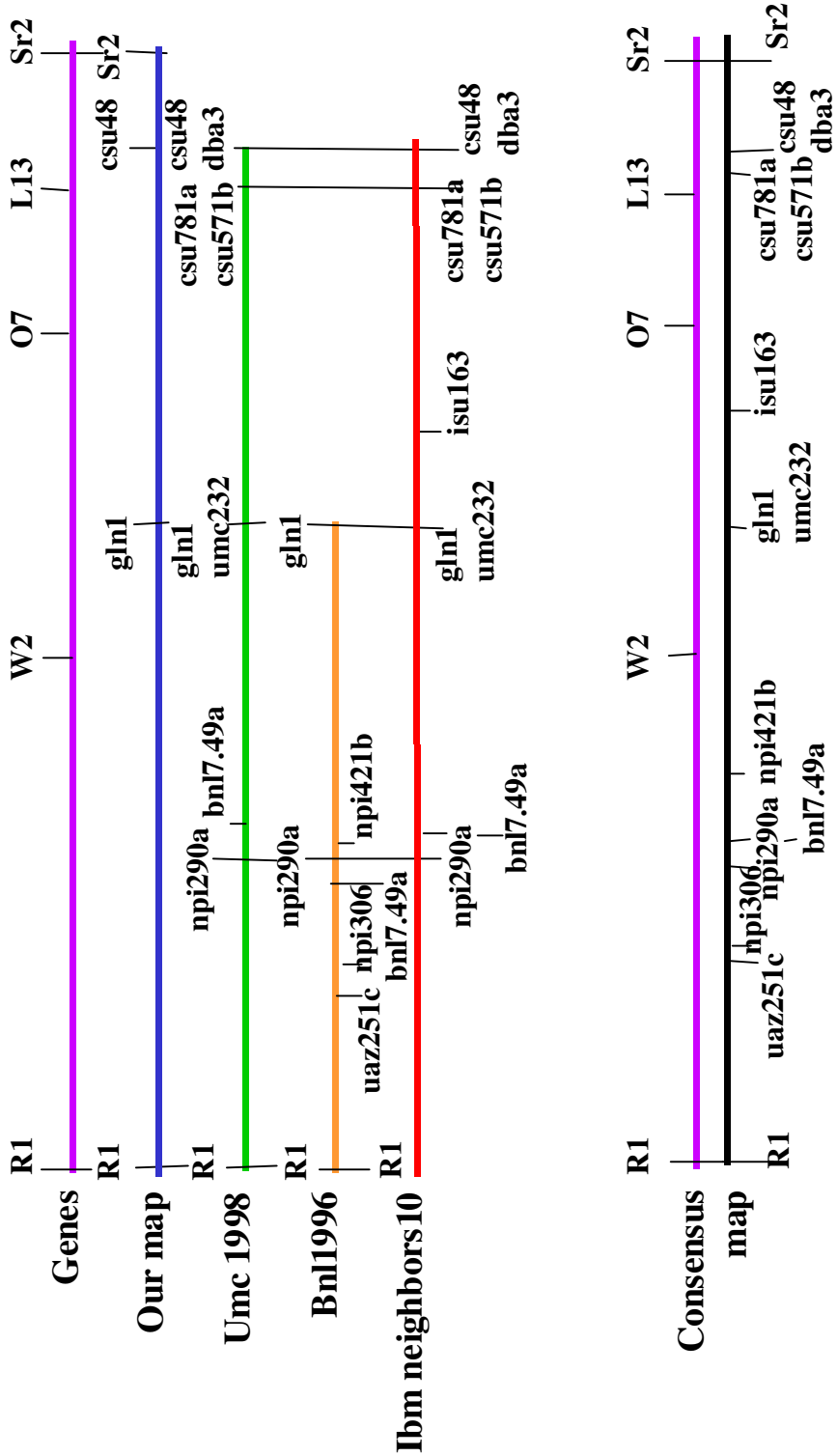
Genes
Our map
Umc 1998
Bnl1996
Ibm neighbors10
Consensus map
R1
W2
O7
L13
Sr2
csu48
dba3
csu781a
csu571b
gln1
umc232
isu163
npi290a
bnl7.49a
npi421b
npi306
uaz251c

FIGURE 2.4: Autoradiographs of RFLP analysis on Ab10. Each image shows the genotypes N10, Ab10, Df-C, Df-I, Df-F, Df-H, Df-K, and Df-L which are labeled at the top of each lane. A. The uaz251 probe shows a polymorphic band that is polymorphic in Ab10, and present in each deficiency examined. B. The polymorphic csu571b fragment reappears in the Df-I genotype and is maintained throughout the larger chromosomes. C. The csu48 RFLP fragment reappears in the Df-F genotype. D. The npi421b RFLP fragment reappears in the Df-H genotype.

A. uaz251c

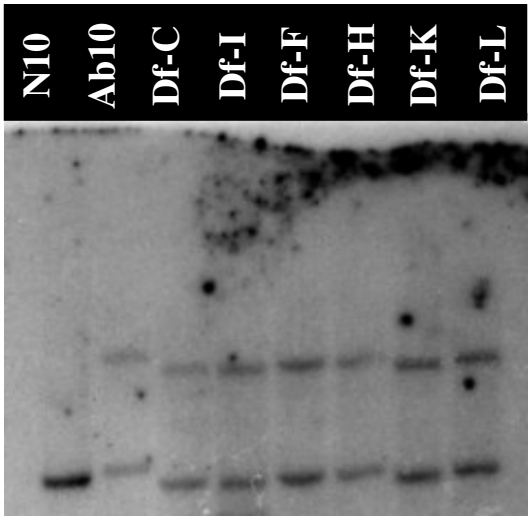

B. csu571b

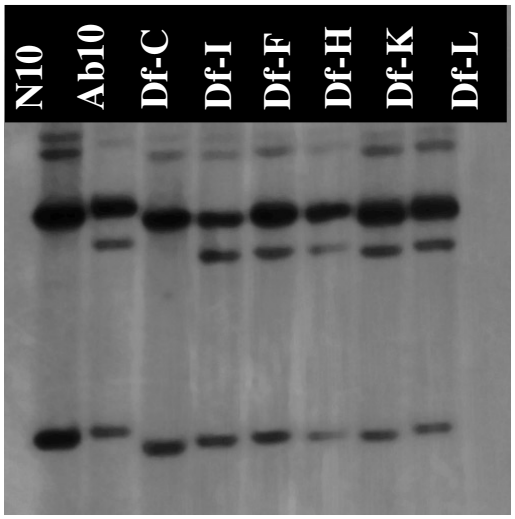

C. csu48

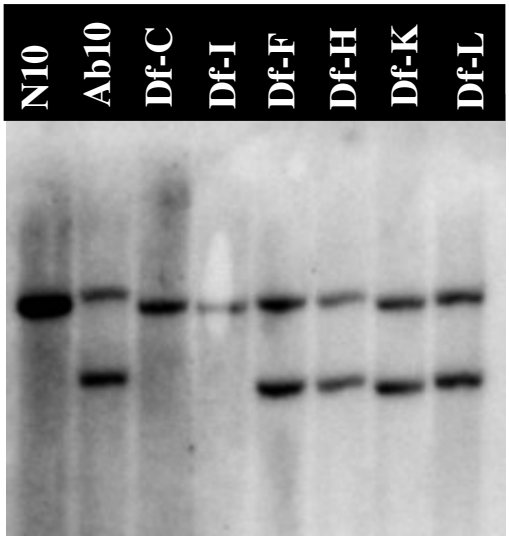

D. npi421b

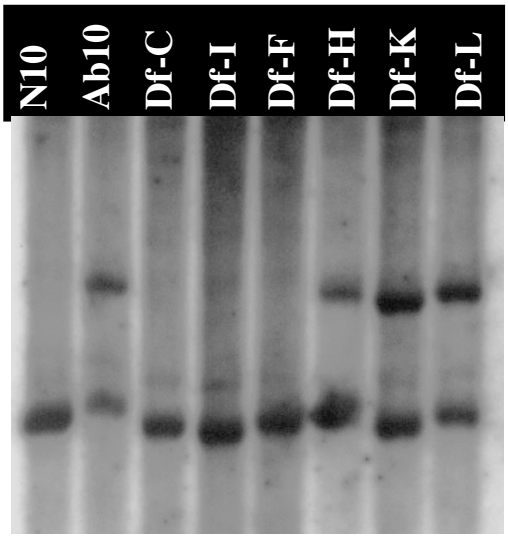

FIGURE 2.5: Comparison of the N10 and Ab10 molecular maps. The consensus N10 map from Figure 2.3 is shown above the Ab10 RFLP map. A blue arrow indicates the proximal location of the csu781a locus and the other proximal RFLP markers bnl7.49a, npi290a, npi 306 and uaz251c. The rearranged regions are shown in brackets, the minor rearrangement is shown in red, the larger, major inversion is bracketed in blue.

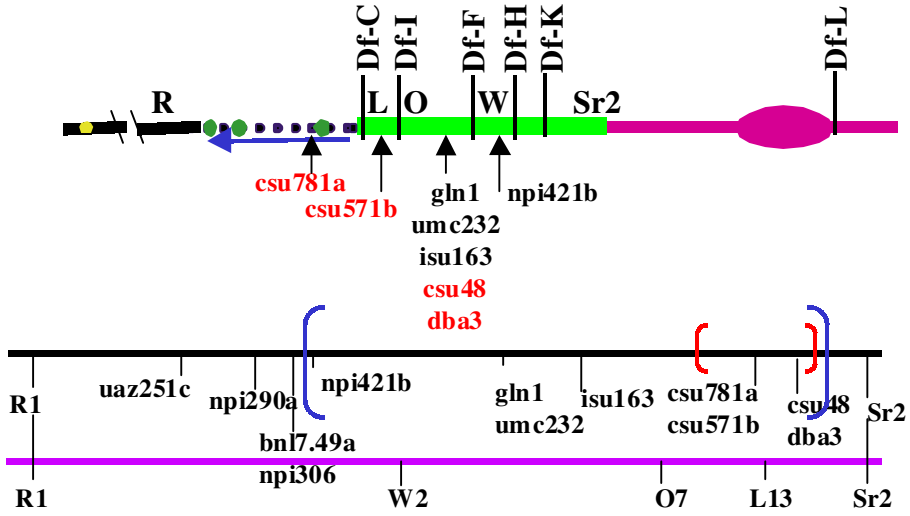
Df-C
Df-I
Df-F
Df-H
Df-K
Df-L
R
L
O
W
Sr2
csu781a
csu571b
gln1
umc232
isu163
csu48
dba3
npi421b
R1
uaz251c
npi290a
bnl7.49a
npi306
W2
gln1
umc232
isu163
csu781a
csu571b
csu48
dba3
Sr2
R1
O7
L13
Sr2

FIGURE 2.6: Model of chromosomal rearrangements from N10 to Ab10. The model involves two separate inversions, and the order of the csu781a and csu571b markers have been assumed in order to simplify the model. One inversion, bracketed in red, begins proximal to csu781 and extends distally to include the csu48/dba3 markers resulting in the intermediate map. Another, larger inversion, bracketed in blue, has a boundary just proximal to npi421b and extends distally to between the csu781 marker and the *Sr2* locus. These rearrangements create the organization of genes and RFLP markers observed on Ab10.

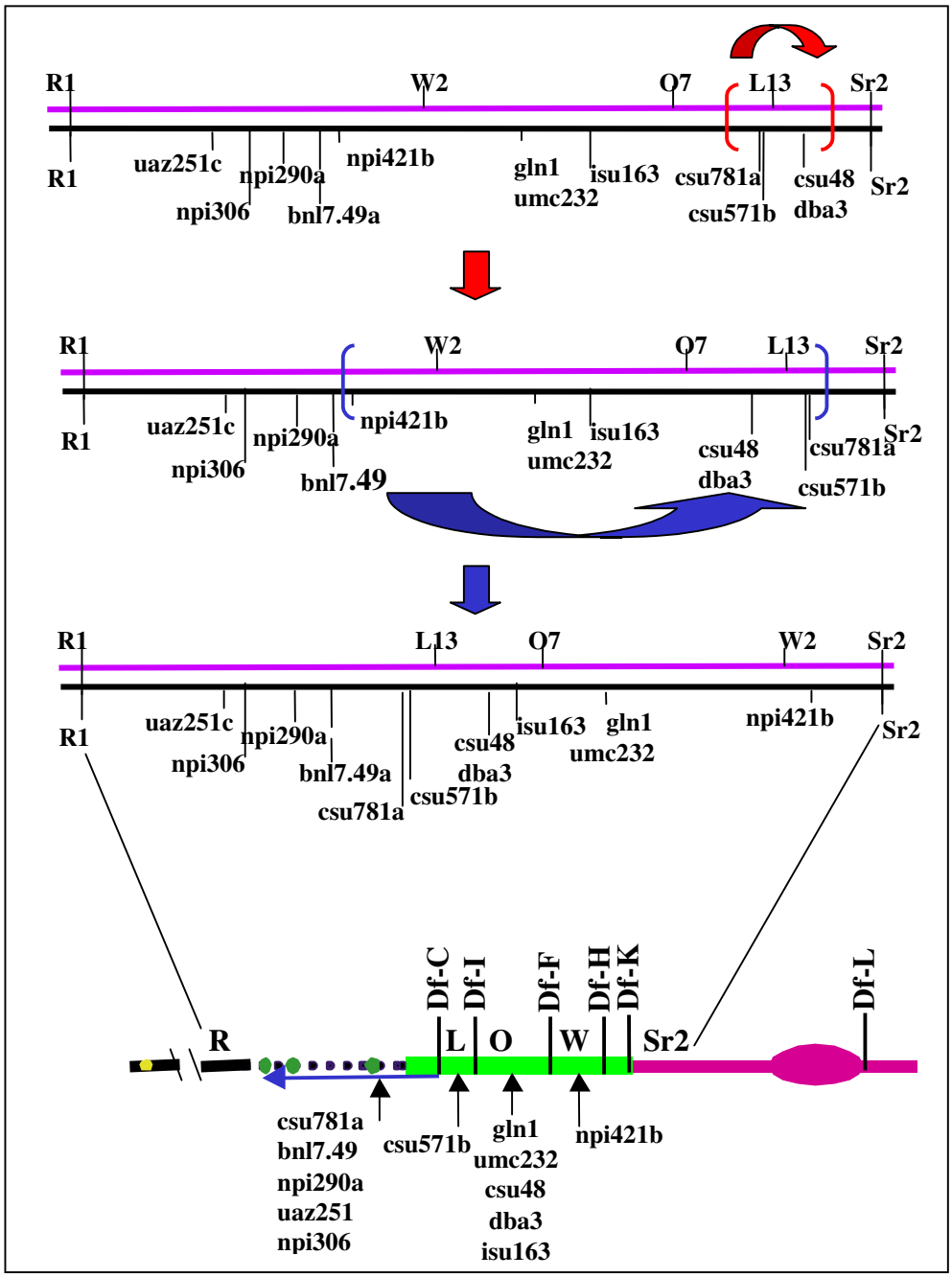
R1
W2
O7
L13
Sr2
R1
uaz251c
npi290a
npi421b
gln1
isu163
csu781a
csu48
Sr2
npi306
bnl7.49a
umc232
csu571b
dba3
R1
W2
O7
L13
Sr2
R1
uaz251c
npi290a
npi421b
gln1
isu163
csu48
csu781a
Sr2
npi306
bnl7.49
umc232
dba3
csu571b
R1
L13
O7
W2
Sr2
R1
uaz251c
npi290a
csu48
isu163
gln1
npi421b
Sr2
npi306
bnl7.49a
dba3
umc232
csu781a
csu571b
Df-C
Df-I
Df-F
Df-H
Df-K
Df-L
R
L
O
W
Sr2
csu781a
bnl7.49
npi290a
uaz251
npi306
csu571b
gln1
umc232
csu48
dba3
isu163
npi421b

CHAPTER 3

DISTRIBUTION OF RETROELEMENTS IN CENTROMERES AND NEOCENTROMERES OF MAIZE[1]

[1] Mroczek, R. J. and Dawe, R. K. Accepted by *Genetics.*
Reprinted here with permission of publisher, 06/20/03

Abstract

Fluorescent in situ hybridization was used to examine the distribution of six abundant long terminal repeat (LTR) retroelements, *Opie*, *Huck*, *Cinful-1*, *Prem-2/Ji*, *Grande*, and *Tekay/Prem-1* on maize pachytene chromosomes. Retroelement staining in euchromatin was remarkably uniform, even when we included the structurally polymorphic abnormal chromosome 10 (Ab10) in our analysis. This uniformity made it possible to use euchromatin as a control for quantitative staining intensity measurements in other regions of the genome. The data show that knobs, known to function as facultative neocentromeres when Ab10 is present, tend to exclude retroelements. A notable exception is *Cinful-1* which accumulates in TR-1 knob arrays. Staining for each of the six retroelements was also substantially reduced in centromeric satellite arrays, to an average of 30% of the staining in euchromatin. This contrasted with two previously described centromere-specific retrotransposable (CR) elements that were readily detected in centromeres. We suggest that retroelements are relatively rare in centromeres because they interrupt the long satellite arrays are thought to be required for efficient centromere function. CR elements may have evolved mutualistic relationships with their plant hosts: they are known to interact with the kinetochore protein CENH3 and appear to accumulate in clusters, leaving long satellite arrays intact.

Transposable elements are divided into two major groups: Class II elements, that transpose through DNA replication, and Class I elements that transpose via an RNA intermediate. Class I transposable elements include LINEs, SINEs, and LTR (long terminal repeat) retroelements. The latter comprise a significant portion of large plant genomes like that of maize, where intergenic regions are composed primarily of nested LTR retrotransposons (SANMIGUEL and BENNETZEN 1998; SANMIGUEL et al. 1996). Roughly 50% of the maize, rye, barley, and wheat genomes are thought to be composed of LTR retroelements (MEYERS et al. 2001; PEARCE et al. 1997; SANMIGUEL and BENNETZEN 1998; SANMIGUEL et al. 1996; VINCENT et al. 1999; WICKER et al. 2001). The same variety of transposable elements appears to exist in smaller-genome species such as rice and *Arabidopsis,* but fewer representatives of each class are present. Only about 14% of the *Arabidopsis* genome is composed of transposable elements (*ARABIDOBSIS* GENOME INITIATIVE 2000). The fact that genome size varies greatly while gene number varies little (the C-value paradox; (CAVALIER-SMITH 1978; PAGEL and JOHNSTONE 1992), can be largely attributed to extraordinary variation in the number of retroelements (BENNETZEN 2002; KUMAR and BENNETZEN 1999; TIKHONOV et al. 1999; WICKER et al. 2001).

LTR retroelements are separated into two major groups based on the organization of the domains within their *Pol* genes; in the Ty1/*copia*-like group the integrase (INT) domain is located upstream of the reverse transcriptase (RT) domain, while in the Ty3/*gypsy*-like group the INT domain is located downstream of the RT domain (XIONG and EICKBUSH 1990). The two groups can be further subdivided into families based upon similarity of their LTR sequences, which evolve faster than the internal coding regions

(SANMIGUEL and BENNETZEN 1998). The distribution of *gypsy*- and *copia*-like LTR retroelements has been analyzed in a number of large genome plants via fluorescent in situ hybridization (FISH) (BRANDES et al. 1997; FRIESEN et al. 2001; KUMAR et al. 1997; PEARCE et al. 1996a; PEARCE et al. 1996b). The patterns of localization suggest that retroelements have insertional preferences. Ty1/*copia* retroelements are found throughout the euchromatin of *Vicia faba* (PEARCE et al. 1996a) but generally concentrated in the sub-telomeric heterochromatin of *Allium cepa* (KUMAR et al. 1997). There is also evidence from *Allium* and gymnosperms that individual retroelement families have discernibly different patterns of chromosomal localization (FRIESEN et al. 2001; PICH and SCHUBERT 1998).

Although most retroelements are distributed non-randomly throughout chromosomes, the most obvious discontinuities occur with respect to tandem repeat arrays. Brandes and coworkers (1997) examined a variety of organisms (*Allium cepa, Beta vulgaris, Brassica campestris, Brassica oleracea, Pennisetum glaucum, Pinus elliottii, Selaginella apoda, Vicia faba* and *Vicia narbonensis*) and demonstrated that the Ty1/*copia* group is dispersed throughout the euchromatic regions, but absent from regions where specialized tandem repeats are expected to lie, such as centromeres, telomeres, heterochromatin, and the NOR. FISH analyses in maize using portions of the *Opie* and *Prem-2/Ji* retroelements showed diffuse patterns of staining with reduced accumulation at the centromeres and NOR (ANANIEV et al. 1998a; EDWARDS et al. 1996; MILLER et al. 1998). In marked contrast are the *gypsy*-like centromeric retrotransposable (CR) elements of cereal grains, which accumulate specifically in centromeric satellites (HUDAKOVA et al. 2001; JIANG et al. 1996; NAGAKI et al. 2003a; PRESTING et al. 1998;

ZHONG et al. 2002). Recent data indicate that the maize CR elements interact with the kinetochore protein Centromeric Histone H3 (CENH3) (ZHONG et al. 2002), suggesting that they participate in centromere function.

Here we describe and quantify the accumulation patterns of a variety of maize retroelement families from both the Ty3/*Gypsy* and Ty1/*Copia* groups, including two different types of maize centromeric retrotransposable (CR) elements. We find that both the *Gypsy* and *Copia* groups are found throughout the euchromatic portions of the genome. In contrast, all but one of the retroelements analyzed are underrepresented in knobs, which are known to function as facultative centromeres. Additionally, all of the retroelements outside of the CR clade are largely excluded from centromeric satellite arrays. The data suggest that centromeric satellite arrays are under selection for their function in chromosome movement, much like genic regions (SANMIGUEL et al. 1996).

Materials and Methods

Maize stocks

The standard maize inbred lines W23 and KYS were used for the bulk of the cytological analysis. The strain containing Ab10 was originally obtained from Marcus Rhoades and subsequently back-crossed into the W23 background 7 times.

Phylogenetic analysis

Nucleotide sequences were retrieved from GenBank for the following maize retroelements: *Grande* 1-4 (GenBank X97604), *Huck* (AF391808 -1), *Tekay* (AF050455), *Fourf* (AF050436), *Mare 5* (AB033252.1), *Reina* (U69258), *Rle*

(AF057037), *Cinful-1* (AF049110), *Cinful*-2 (AF049111), *Prem-2* (U41000), *Opie*-2 (U68408), *Cent-A* (AF078917), CRM (AY129008), CRR (AC022352), *Cereba* (AY040832) and two *Arabidopsis thaliana* retroelement sequences (AAD11616 and BAB40826). The reverse transcriptase regions were identified following the guidelines set forth by Xiong and Eickbush (XIONG and EICKBUSH 1990). A progressive alignment of the RT regions was prepared using the Pileup option in GCG' Seqlab with a BLOSUM 30 transition matrix (FENG and DOOLITTLE 1987; GCG 1982-2000; HENIKOFF and HENIKOFF 1992). The alignments were adjusted manually using previously published RT alignments as visual templates (BOWEN and MCDONALD 2001; XIONG and EICKBUSH 1988). Both parsimony heuristics and Neighbor-Joining were used to generate trees from our alignment using PAUP* (SWOFFORD 1999). The NJ trees were derived using uncorrected pairwise distances (SWOFFORD 1999), and Bootstrap values were determined using PAUP*.

Probe preparation

Primers specific to LTRs were designed from the sequences noted above with the exceptions of *Huck* (AF050438) and *Grande* (AF050437). The lengths of the amplified products, and the primers used for the amplification, are as follows. *Cinful-1*: 562 bp (F- 5' -CGCCGAAGGTCTTCTAGGAA-3' R- 5' -GGAGACTCGTTCTCAAGTGCTA-3'); *Grande*: 350 bp (F- 5' -ATGCGAGGATAAGTCGGCGAAG-3' , R- 5' -GGTGTTTTTAGGAGTAGGACGGTG-3');*Huck*: 673 bp (F- 5' -TCCACTGACCGACCTGACAA-3' , R- 5' -GGTTTTGGCACCCTGTTCAT-3'*Opie-2*: 526 bp (F- 5' -CAAACACAAGTGCTTAAAT-3' , R- 5' -GTCCGGTGCCCGATTTGT-3');

Prem-2/Ji: 573 bp (F- 5' -ACATTTGGTGGTTGGGGCTA-3' , R- 5' -GGGTGAATAGGGCGAAACTGAA-3'); and *Tekay*: 537 bp (F- 5' -ATTTGTGCGACCGCTCAA-3' , R- 5' -AGGAGTCCAGGCTGCTCTTA-3'); *Cent-A*: 1234 bp (F – 5'-CATAACCCGCACAGATATGAC-3' R- 5'-ATAAACCCAACGGGTAGAAGGG-3' ; and CRM: 513 bp (F- 5' -TCGTCAACTCAACCATCAGGTGAT-3' , R- 5' -GCAAGTAGCGAGAGCTAAACTTGA-3'). The PCR fragments were each cloned into the TOPO cloning vector (Invitrogen, Carlsbad, CA) and verified by sequencing.

In Situ Hybridization

Anthers from maize inbred lines were fixed as previously described (HIATT et al. 2002). Probes were amplified from plasmids and labeled with FITC using a random primer labeling kit (Prime-It Fluor Fluorescence Labeling Kit, Stratagene, La Jolla, CA). The CentC and TR-1 repeats were detected using rhodamine-labeled oligonucleotides specific to each sequence (HIATT et al. 2002; ZHONG et al. 2002). Chromosome straightening and in situ hybridization was carried out as previously described (DAWE et al. 1994; ZHONG et al. 2002). All data were collected and analyzed using a DeltaVision 3D light microscope workstation and associated software. Intensity data was collected by first selecting 9 X 9, two-dimensional 'pixel boxes'. From these boxes we recorded the total intensity values (amount of light detected by the CCD camera in that region) from the DNA (DAPI) and retroelement (FITC) channels. Background, euchromatin, centromere, and knob readings were taken in each channel for each cell. Background measurements were averaged from 5 different pixel boxes and euchromatin

measurements averaged from 10 different pixel boxes. For knobs and centromeres the number of pixel boxes for which data was collected was limited by the number of centromeres or knobs that were unobstructed by chromosome arms; between 4 and 7 pixel boxes were taken for each structure in each cell. The pixel box data from each channel were averaged, and appropriate background levels subtracted for each cell. The overall intensity values varied from cell to cell, as is typical for FISH experiments. We therefore calculated within-cell ratios of centromere/euchromatin or knob/euchromatin staining intensities for both channels and compared them. By taking advantage of an internal control (euchromatin staining) we effectively normalized the data, making it possible to average the information from different cells.

Results

Phylogeny of the retroelement families analyzed: We identified the reverse transcriptase (RT) regions of the retroelements examined in this report and compared their sequences to several other retroelements phylogenetically. Neighbor-Joining and parsimony analysis of the retroelement RT regions produced identical trees. Figure 3.1 is a Neighbor-Joining tree which shows that the retroelements can be divided into two major clades representing the *gypsy*- and *copia*-like groups of the LTR retroelements, a finding that is consistent with other phylogenetic analyses (BOWEN and MCDONALD 2001; MALIK and EICKBUSH 1999; XIONG and EICKBUSH 1990). The known CR elements group together to form a monophyletic clade within the *gypsy*-like group (LANGDON et al. 2000; NAGAKI et al. 2003a). In maize there are two different CR elements, CRM and *Cent-A*, which have closely related internal regions (67% nucleotide

similarity) but completely different LTRs (ANANIEV et al. 1998a; ZHONG et al. 2002). Among the known maize retroelements, *Tekay/Prem-1* and *Reina* are the most closely related to the CR elements. However, only *Tekay/Prem-1* is abundant enough (MEYERS et al. 2001; SANMIGUEL and BENNETZEN 1998) to be readily detected by FISH.

The abundant maize retroelement families show genome-wide distributions: We chose six of the most abundant maize retrotransposon families for in situ hybridization analysis — *Huck*, *Opie*, *Grande*, *Prem-2/Ji*, *Cinful-1*, and *Tekay/Prem-1* (MEYERS et al. 2001; SANMIGUEL and BENNETZEN 1998; SANMIGUEL et al. 1996). Probes were generated to portions of the LTRs that are unique to individual families. These LTR fragments were then flourescently labeled, hybridized to maize pachytene chromosome preparations, and the results analyzed using deconvolution 3D light microscopy. Each of the retroelement families outside of the CR clade showed roughly uniform euchromatic staining patterns throughout the genome (FIGURES 3.2 and 3.3), with subtle differences among families. *Opie* is evenly distributed in a pattern of neat dots along the chromosomes (FIGURE 3.3); *Huck* has a patchy distribution (FIGURE 3.3); and *Prem-2/Ji* has a genome-wide distribution but on some chromosomes is underrepresented in pericentromeric heterochromatin (FIGURE 3.2, arrows; FIGURE 3.3).

Retroelement abundance in euchromatic regions is relatively uniform but varies in knobs

Visual inspection of the images in figures 3.2 and 3.3 indicated a remarkable uniformity in the distribution of retroelements along chromosome arms, suggesting that euchromatin staining might serve as a suitable internal control for the staining in centromeric regions. To test this idea, we compared the euchromatin on abnormal

chromosome 10 (Ab10) to other chromosome arms. Ab10 is an alternative version of the normal 10 chromosome that is present in roughly 10% of teosinte (the ancestor of maize) and about 2% of known maize strains (KATO 1976). The terminal portion of the long arm of Ab10 is responsible for the phenomena of neocentromere activity and meiotic drive. This region contains few essential genes (HIATT and DAWE 2003b) and a ~14 map unit inversion (RHOADES and DEMPSEY 1985). In addition there are three small knobs containing arrays of a 350 bp TR-1 knob repeat, and a large knob composed primarily of a 180 bp repeat (ANANIEV et al. 1998b; HIATT et al. 2002; PEACOCK et al. 1981; RHOADES and DEMPSEY 1985). The striking structural polymorphism between Ab10 and the normal chromosome 10 (N10), most notably the inverted region, is thought to be responsible the fact that recombination between the distal portion of Ab10 and N10 rarely occurs (KIKUDOME 1959; RHOADES and DEMPSEY 1985). The unusual structural features and evolutionary history of Ab10 suggested that it might have an unusual distribution or abundance of retroelements.

We assayed the localization patterns of a sample of retroelements (*Huck*, *Prem-2/Ji*, and *Cinful-1)* on the distal portion of the Ab10 chromosome. As can be seen in FIGURE 3.4, retroelement staining in the euchromatic portion of the distal region of Ab10 was nearly identical to the intensity and pattern of staining observed for the rest of the genome. To quantify this observation we took advantage of the fact that chromatin (DAPI) and retroelement (FITC) staining are measured and stored as separate images during data collection, and that deconvolution microscopy is quantitative. Staining intensity readings were taken for both chromatin and retroelements and compared to the staining intensities found in other euchromatic regions. We found no significant

difference between Ab10 and the rest of the genome (*t*-test, $P < 0.01$). Although the DAPI intensity in Ab10 euchromatin was relatively low compared to the genome as a whole (mean = 0.73, SD ± 0.53) retroelement intensities were similarly reduced (mean = 0.77 , SD ± 0.21). These data support the view that retroelements are spread evenly and uniformly throughout maize euchromatin.

Our analysis of Ab10 also revealed that euchromatin and knobs stain differently for retroelements. For instance, *Huck* is nearly absent from the large knob of Ab10 (FIGURE 3.4C), and *Cinful-1* is highly abundant within the TR-1-containing chromomeres (indicated by staining that appears yellow, FIGURE 3.4D). As described below, these observations were pursued in more detail by analyzing a variety of other knobs in the genome.

Retroelement families are variably interspersed in maize knob satellite DNA

The TR-1 and 180 bp repeats present on Ab10 also occur at 22 other knob loci in differing proportions (ANANIEV et al. 1998c; BUCKLER et al. 1999; HIATT et al. 2002; KATO 1976). Many other classes of repeats may also be present in maize knobs. In order to obtain a more general perspective on knobs without a bias towards particular repeats, we scored retroelement staining in knobs as identified by their characteristic ball-shaped heterochromatic structure (FIGURE 3.6, see also FIGURES 3.2 and 3.3). We found that all families except *Huck* showed some staining in nearly every knob observed (FIGURE 3.6). The retroelement families *Cinful-1*, *Grande*, *Tekay/Prem-1*, *Opie*, and *Prem-2/Ji* all showed staining in the majority of knobs examined (84.8%, 86.7%, 87.1%, 94.9% and 96.3% respectively). In contrast, the *Huck* retroelement family was nearly absent in most

knobs with some staining in only 20% of the knobs examined (Table 1). Retroelements from the *Huck* family apparently avoid or are selectively removed from knobs even though they occupy roughly 10% of the maize genome (MEYERS et al. 2001; SANMIGUEL and BENNETZEN 1998). Our observations are consistent with the findings of ANANIEV and coworkers (1998b), who found no copies of the *Huck* retroelement family in any of 23 cloned knob segments.

Probes for retroelements outside of the *Huck* and CR families appeared to stain euchromatin and knobs at about the same intensity (FIGURE 3.6). Since knobs stain with DAPI very brightly, this observation implied a relatively low abundance of retroelements within the knobs. Intensity measurements confirmed the interpretation: we found that knobs were 2.6 times brighter in the DAPI channel than an average segment of euchromatin, but that retroelement staining within knobs was only 1.1 times brighter (FIGURE 3.5). In the small percentage of knobs that showed *Huck* staining, retroelement staining intensities were only 15% of the levels in euchromatin. These data indicate that although most retroelement families are present in the satellite repeats of knobs, they are present there at a reduced frequency when compared to euchromatin.

Data from the Ab10 chromosome indicated that *Cinful-1* retroelements accumulate in TR-1 knobs (FIGURE 3.4D). To determine if *Cinful-1* accumulation was limited to Ab10 knobs, we took intensity readings from the TR-1 knobs of Ab10 as well as three other TR-1 containing knobs. Overall, *Cinful-1* staining was 2.2 times higher in TR-1 knobs than in euchromatin (FIGURE 3.5), and there was no significant difference between the TR-1 knobs on Ab10 and those elsewhere in the genome (*t*-test, $P < 0.01$). In contrast the staining intensities for *Huck* and *Prem-2/Ji* in TR-1 knobs were similar to

those in non-TR-1-containing knobs. The fact that *Cinful-1* is substantially over represented in TR-1 arrays provides evidence that the reduced staining we detect for all the other retroelements is not a consequence of the heterochromatic nature of knobs.

Abundant retroelement families are largely absent from centromeres

Maize centromeres contain tandem arrays of the 156 bp Cent-C satellite repeat, interspersed with the CR elements *Cent-A* and CRM (NAGAKI et al. 2003a; ZHONG et al. 2002). Non-centromere-specific retroelements are also present to some extent, though the overall frequency of these elements in centromeres is not known (ANANIEV et al. 1998a; NAGAKI et al. 2003a) and will be difficult to determine by sequence analysis given the inherent limitations associated with cloning and contiging long repeat arrays (HENIKOFF 2002; SONG et al. 2001). In an effort to further examine and quantify the accumulation patterns of retroelements in centromeres, we labeled the major retroelement LTRs and Cent-C with different fluorescent dyes and analyzed the results on DAPI-stained maize pachytene chromosomes.

We found that each of the retroelement families *Huck*, *Opie*, *Grande*, *Prem-2/Ji*, *Cinful-1*, and *Tekay/Prem-1* are poorly represented at centromeres (FIGURE 3.3, FIGURE 3.5 and Table 1). The percentage of centromeres with detectable staining for these retroelements ranged from 3.4% to 37% depending on the family (Table 1). Similarly, while DAPI staining intensities were roughly equivalent in centromeres and chromosome arms, non-CR retroelement staining in centromeres averaged only 30% of the levels found in euchromatin (FIGURE 3.5).

In marked contrast to other maize retroelement families, in situ hybridization with the CR elements *Cent-A* (ANANIEV et al. 1998a) and CRM (NAGAKI et al. 2003a; ZHONG et al. 2002) revealed strict centromeric localization on all 10 maize chromosomes (FIGURE 3.7, Table 1). We often observed overlap of the CentC and CR signals (FIGURE 3.7, CRM), in many cases the two signals were clearly separate (FIGURE 3.7, *Cent-A*). These data are consistent with fiber-FISH data from rice which suggest that CR elements tend to insert into large clusters distinct from the regions composed mainly of satellite repeats (CHENG et al. 2002).

Discussion

In this study we provide a perspective on the distribution of the most abundant retroelements in maize with particular emphasis on the centromeres and neocentromeres. Previous reports have used general reverse transcriptase probes to examine overall distribution patterns of retroelements (BRANDES et al. 1997; KUMAR et al. 1997; PEARCE et al. 1997; PEARCE et al. 1996a; PEARCE et al. 1996b), or have localized specific families without a special emphasis on centromeres (FRIESEN et al. 2001; PICH and SCHUBERT 1998). Retroelement distribution is also being analyzed in the sequenced plant genomes of *Arabidopsis* and rice (FENG et al. 2002; *ARABIDOPSIS* GENOME INITIATIVE 2000). However, sequence data is generally unreliable in regions containing long satellite arrays (HENIKOFF 2002). Even the size of most eukaryotic centromeres is still under debate (HAUPT et al. 2001; HOSOUCHI et al. 2002). The FISH strategy employed here has a lower resolution than DNA sequencing but can provide a general and quantitative perspective on the frequency of retroelements in large centromeres. By focusing on a

single organism, using retroelement family-specific probes, and using quantitative light microscopy, we have been able to draw new conclusions and hypotheses about the forces driving retrotransposon accumulation in large-genome species.

Chromosomal localization with respect to evolutionary history of the elements

The families examined represent both the *gypsy*- and *copia*-like groups of LTR retroelements. *Huck*, *Cinful-1*, *Tekay/Prem-1*, *Grande*, *Cent-A*, and CRM belong to the *gypsy*-like group and *Prem-2/Ji*, and *Opie* fall into the *copia*-like group. In our analysis of eight retroelement families from maize we saw no obvious correlation between the type of retroelement (*gypsy*- or *copia*-like) and chromosomal localization patterns. The rapid evolution of localization patterns is particularly evident with regard to the CR elements and the closely related *Tekay/Prem-1* retroelement family. Although *Tekay/Prem-1* shares a more recent common ancestor with the CR elements than do the other families examined here, it is no more likely to be found in or near the centromere than more distantly related families. As can be seen in Table 1 and figure 3.5, the *Cinful-1 and Opie* families are just as likely to show centromeric staining as the *Tekay/Prem-1* family. The available data suggest that the strict centromeric localization pattern and apparent functions of CR elements in recruiting centromeric histone are recently-evolved features primarily limited to the cereal grains.

Accumulation of retroelements in Ab10 and the satellite repeats of maize knobs

The abnormal 10 chromosome of maize provides all knobs in the genome with the capacity to move as neocentromeres and preferentially segregate to progeny (RHOADES

1942). Within the terminal region of the long arm of Ab10 there is an inversion of chromatin from normal 10, three small knobs composed primarily of TR-1 repeats, a large knob composed primarily of 180 bp repeats, and regions of apparently novel chromatin (HIATT et al. 2002). Genetic data suggest there are few essential genes in the later half of this large structural polymorphism (HIATT and DAWE 2003b). Meiotic drive systems may spread to some extent without regard to organismal fitness, and are known to accumulate deleterious mutations (ARDLIE 1998). Similarly, retroelements have been shown to accumulate in *Drosophila* inversions, presumably because recombination events that would eliminate them are reduced there (SNIEGOWSKI and CHARLESWORTH 1994). Because of its association with meiotic drive, reduced recombination, and relative lack of genes, we considered whether the distal portion of Ab10 would be a favored spot for the accumulation of retroelements. However, outside of the *Cinful-1* family which accumulates in all TR-1 arrays, the retroelement families we examined appear to be no more abundant on this chromosome than they are throughout the rest of the genome (FIGURE 3.4). These data suggest that the reduced recombination and meiotic drive typical of the long arm of Ab10 have had little impact on retroelement distribution over the time span that the drive system has existed (see BUCKLER et al. 1999).

The remarkable uniformity of retroelement distribution in maize euchromatin gave us a useful internal control for the staining of retroelements in knobs and centromeres. The analysis indicates that retrotransposons are substantially underrepresented in knobs relative to euchromatin (FIGURE 3.4, FIGURE 3.5). One explanation for the under representation of retroelements in knobs is that the structural organization of knob heterochromatin is such that FISH probes cannot gain access.

However, the fact that we detected an abundance of *Cinful-1* elements in TR-1 arrays strongly suggests that knob structure did not serve as a substantial barrier to FISH probes. In addition we have corroborated a previous conclusion, based on the analysis of cosmid clones, that *Huck* is underrepresented in knobs (ANANIEV et al. 1998b). We believe our data provide an accurate view of the prevalence of retroelements in knob repeat arrays.

The fact that retroelements are underrepresented in knobs indicates that long tracts of tandem repeats may be required for neocentromere function, as argued below for centromeres. Although there are clearly more retroelements in knobs than in centromeres (FIGURE 3.5), this may reflect the fact that neocentromeres are only activated when Ab10 is present, and as a result there are less stringent evolutionary restraints upon the content of knobs. Interestingly, TR-1 satellite arrays are considerably more neocentric (active on the spindle) than 180 bp arrays, and are controlled by different transacting factors (HIATT et al. 2002). Our data suggest that *Cinful-1* does not actively interfere with TR-1-mediated neocentromere activity and leaves open the possibility that *Cinful-1* may contribute to knob motility, as has been suggest for the CR elements (ZHONG et al. 2002).

Abundance of maize retroelements in centromeres

An unusual feature of cereal centromeres is that they specifically accumulate a group of Ty3-*gypsy*-like retroelements known as CR elements. CR elements show remarkable sequence conservation and are found in the centromeres of rice, wheat, sorghum, barley , rye and oats (ARAGON-ALCAIDE et al. 1996; JIANG et al. 1996; LANGDON et al. 2000; MILLER et al. 1998; PRESTING et al. 1998). Zhong and coworkers have recently reported that maize CR elements interact with the centromeric histone

CENH3, indicating that they may have been co-opted to perform a function in chromosome segregation (ZHONG et al. 2002). The strict centromeric localization of CR elements is even more striking in light of data shown here that several other maize retroelement families are poorly represented within centromeres, at least as defined by co-localization with the CentC satellite repeat. CentC strongly interacts with the kinetochore protein CENH3, suggesting that it is a legitimate marker for the functional centromere (ZHONG et al. 2002). *Cent-A* and CRM are abundant in centromeres (FIGURE 3.7), whereas retroelements that occur throughout the chromosome arms (*Grande*, *Opie*, *Prem-2/Ji*, *Huck*, *Cinful-1* and *Tekay/Prem-1*) are significantly underrepresented in centromeres (FIGURES 3.2, 3.3, and 3.5, Table 1). There is some family-to-family variation, but overall the non-CR retroelements are found 3-fold less frequently in centromeres than in euchromatin. The tandem repeats in maize centromeres apparently represent a niche of the genome that is favorable to CR elements, and seemingly hostile to families of retroelements that proliferate throughout the intergenic, euchromatic niches of the genome.

Extended tandem repeat arrays are thought to be required for centromere function in animals (GRIMES et al. 2002), and are characteristic of the centromeres in *Arabidopsis* and rice (CHENG et al. 2002; KUMEKAWA et al. 2001). Rampant insertion of retroelements in the centromere would interrupt the continuity of these long arrays. Based on our data, we hypothesize that such insertions adversely impact the formation of centromeric chromatin. Other functional domains of the chromosome, most notably those containing genes, also rarely contain the large insertions that retrotransposons generate (SANMIGUEL et al. 1996). Non-CR retrotransposons may be excluded from the

centromere by the chromatin structure at the centromere, or alternatively, could be eliminated during the process of unequal crossing-over that is thought to homogenize tandem repeat arrays (EICKBUSH 2002). The CR elements may circumvent elimination via recombination by continuously transposing back into the centromeric satellite arrays, as has been proposed for the maintenance of R1 and R2 elements in *Drosophila* rRNA gene arrays (EICKBUSH 2002; PEREZ-GONZALEZ and EICHBUSH 2002). This interpretation is supported by sequencing data showing that most CR elements are recent insertions (NAGAKI et al. 2003a). Further, fiber-FISH analyses (CHENG et al. 2002), and our own localization data (FIGURE 3.7) suggest that CRs transpose into specific domains of the centromere, leaving the tandem repeat arrays largely intact.

At least a subset of known retroelements seem to have evolved mutualistic relationships with their hosts. Two particularly well-studied examples in this category are the HeT-A and TART elements of *Drosophila*, which substitute for telomerase by continually transposing into chromosome ends (PARDU and DEBARYSHE 2000). Although the host normally responds to retroelements by actively repressing them, *Drosophila* may tolerate HeT-A and TART because it benefits from their presence. Similarly, CR elements accumulate in specific domains of the centromere where they interact with the key kinetochore protein CENH3 (ZHONG et al. 2002). These data suggest that CR elements contribute to the specification and/or maintenance of the centromere/kinetochore complex. In the same manner that HeT-A and TART elements are limited to *Drosophila* species (CASACUBERTA and PARDU 2003), the CR elements and their association with centromeres may be limited to cereal grains. There are no *Arabidopsis* retroelements that transpose specifically into the centromere core (HAUPT et

al. 2001; KUMEKAWA et al. 2001) and chromatin immunoprecipitation experiments have failed to reveal any association between retroelements and the *Arabidopsis* homologue of CENH3 (NAGAKI et al. 2003b). The functional centromeric sequences in *Arabidopsis*, as in humans (GRIMES et al. 2002; SCHUELER et al. 2001), appear to be long uninterrupted arrays of satellite repeats (NAGAKI et al. 2003b).

Table 1. Presence of retroelements at centromeres and knobs

Retrolement	Total centromeres counted	% Centromeres with detectable staining	Total knobs counted	% Knobs with detectable staining[a]
Opie	19	26.3	39	94.9%
Prem-2/Ji	58	3.4	80	96.3%
Cinful-1	27	37.0	46	84.8%
Grande	13	15.4	15	86.7%
Tekay/Prem-1	31	22.6	31	87.1%
Huck	30	6.7	40	20.0%
Cent-A	32	100.0	[b]	[b]
CRM	60	100.0	[b]	[b]

[a] Number of knobs observed for which retroelement staining was at least as intense as that observed throughout the euchromatin of the chromosomes.

[b] Cent-A and CRM are not detected at knobs or euchromatin.

FIGURE 3.1: Neighbor-Joining tree of the reverse transcriptase (RT) amino acid sequences from a variety of plant retroelements. AAD11616 and BAB40826 represent RT sequences from *Arabidopsis*. CRM and *Cent-A* are CR elements from maize. CRR and *Cereba* are CR elements from rice and barley respectively. All other retroelements are from maize. Numbers at the nodes represent the bootstrap values obtained using PAUP*.

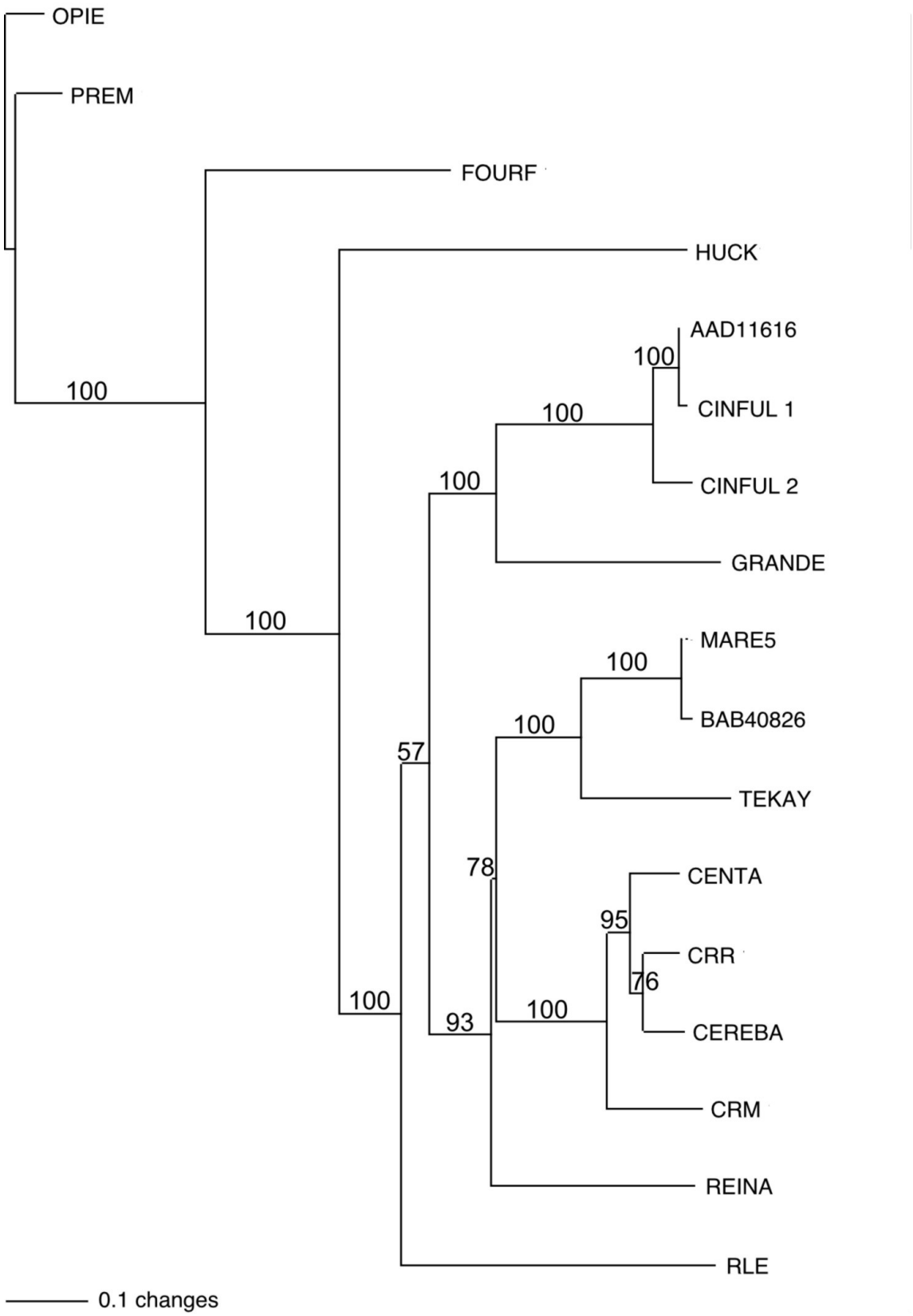
OPIE
PREM
FOURF
HUCK
AAD11616
CINFUL 1
CINFUL 2
GRANDE
MARE5
BAB40826
TEKAY
CENTA
CRR
CEREBA
CRM
REINA
RLE
100
100
100
100
100
100
57
78
95
76
100
93
100
0.1 changes

FIGURE 3.2: Genome-wide distribution of the *Prem-2/Ji* retroelement family in maize. Images are single optical sections taken from a maize pachytene meiocyte, separated by 4 μm. DNA is represented in magenta and the *Prem-2/Ji* retroelement family is represented in green. Absence of *Prem-2/Ji* staining at centromeres is indicated with red arrowheads. *Prem-2/Ji* staining at a knob is shown with a white arrowhead.

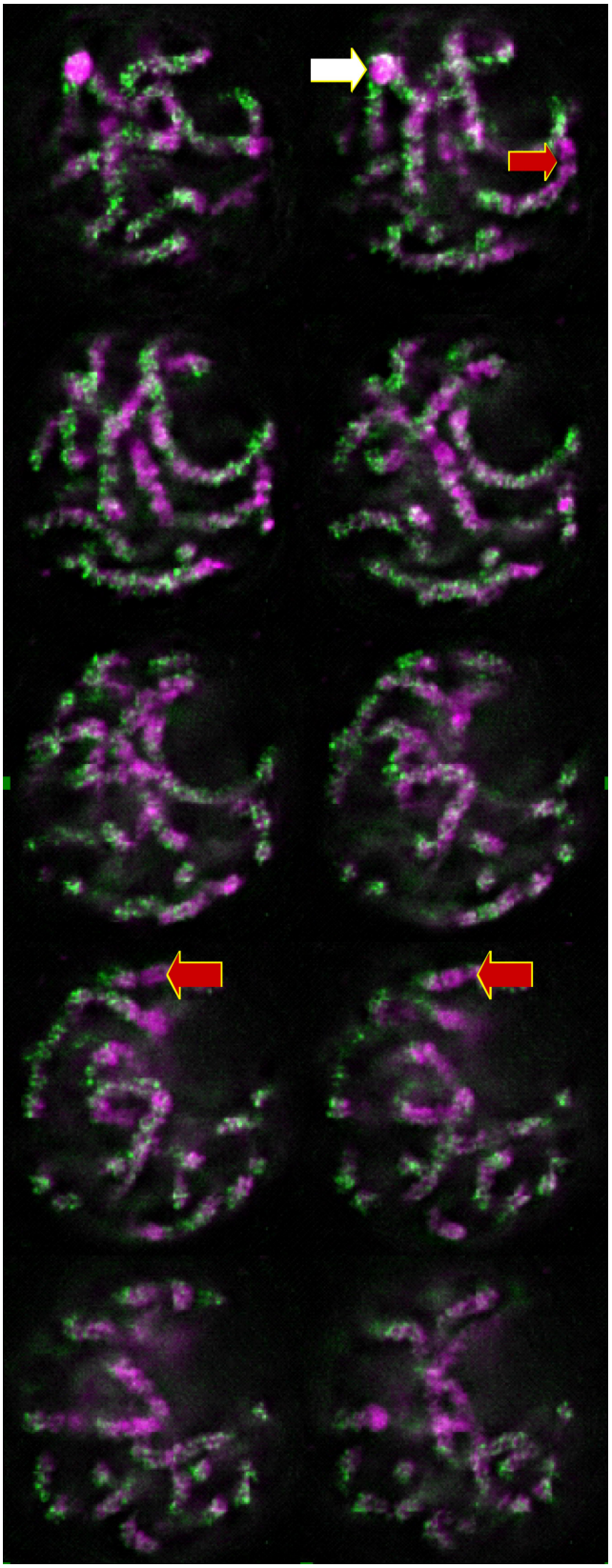

FIGURE 3.3: Staining patterns of maize retroelement families throughout the genome with respect to the centromeres**.** Each image shows a single optical section of a cell at pachytene. DNA is shown in blue, CentC in green, and retroelement LTR staining in red. (A, C) 2X Enlargements of the boxed areas showing retroelement staining around the centromere. (B, D) Same images as A and C, except with the CentC staining removed.

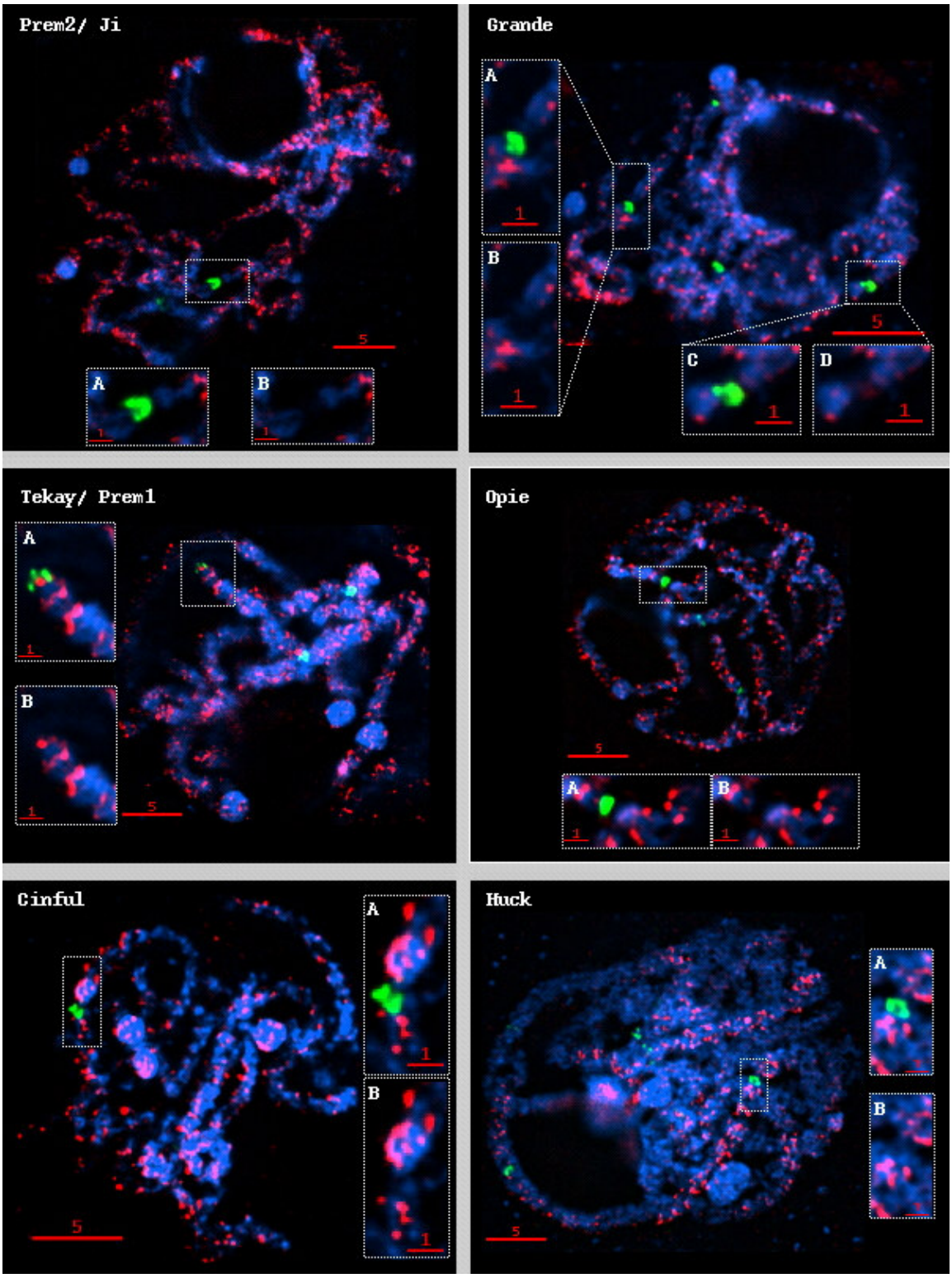
Prem2/ Ji
A
B
Grande
A
B
C
D
Tekay/ Prem1
A
B
Opie
A
B
Cinful
A
B
Huck
A
B

FIGURE 3.4: Staining patterns of retroelements in the polymorphic portion of Ab10. (A) Graphical representation of the Ab10 chromosome showing the small TR-1 knobs in green, the large 180 bp repeat knob in blue, and the euchromatic regions in purple. (B) Black and white image of a computationally straightened Ab10 chromosome showing only DNA (DAPI) staining; chromomeres are indicated with connecting lines to the graphical representation in A. (C) *Huck* staining on a computationally straightened Ab10 pachytene chromosome. TR-1 staining is in green and retroelement staining in red. (D) Straightened chromosome from a cell stained with *Cinful-1* in red and TR-1 in green. Intense *Cinful* staining at the TR-1 knobs makes them appear yellow, due to the overlap of the red and green colors. (E) Straightened chromosome showing *Prem-2/Ji* in red and TR-1 in green.

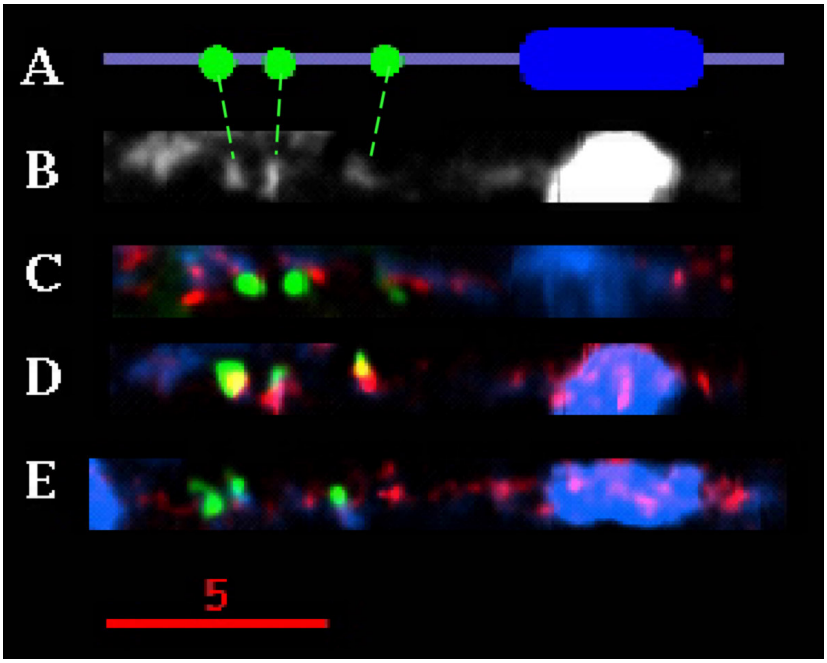
A
B
C
D
E
5

FIGURE 3.5: Staining intensities of DNA and retroelements in centromeres, cytologically-defined knobs, and TR-1 arrays. Staining intensities are expressed relative to euchromatin. Values below the bold dashed line indicate relatively low staining intensities, values above the line indicate high staining intensities. SD = standard deviation.

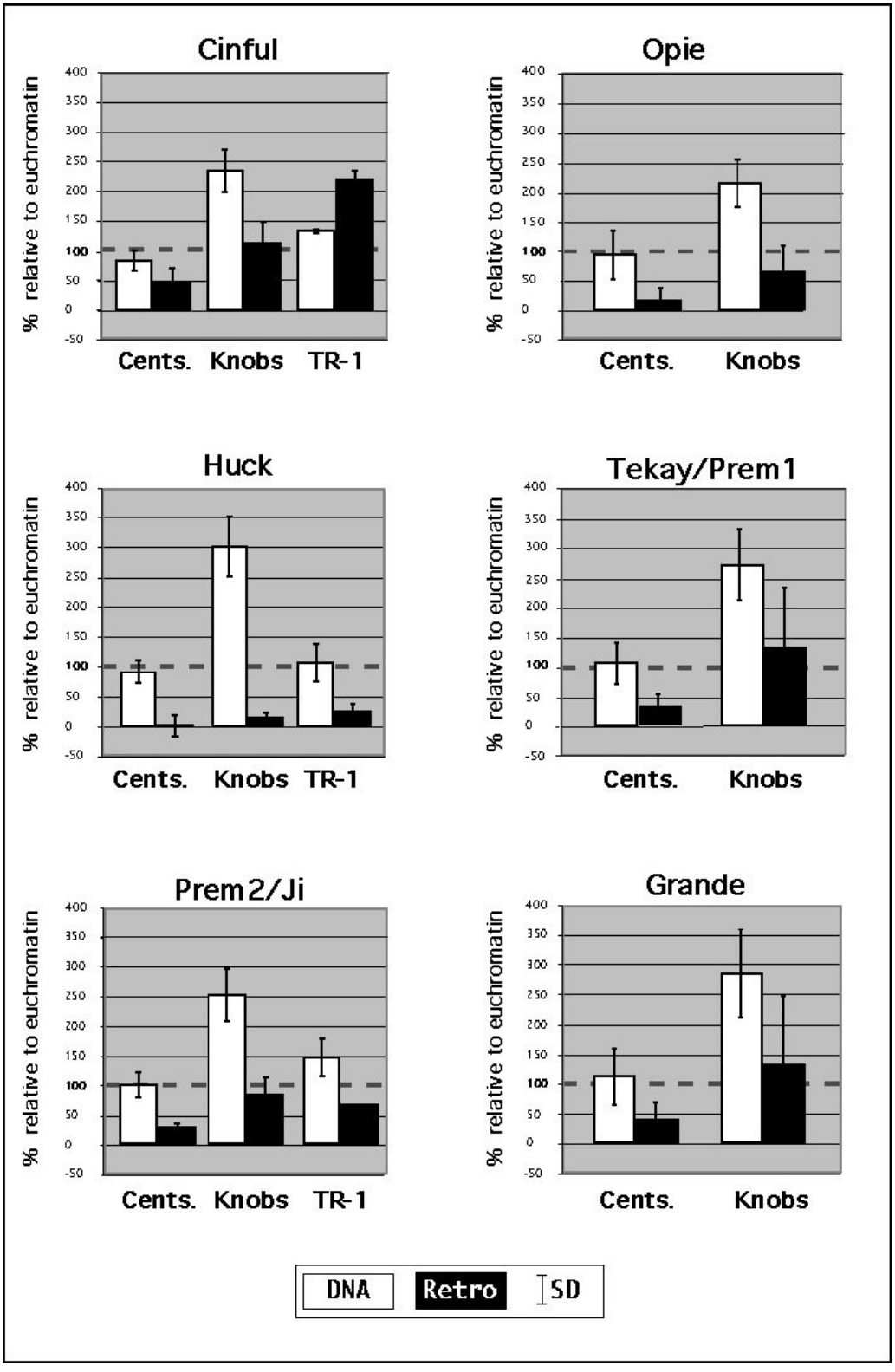
Cinful
Opie
Huck
Tekay/Prem1
Prem2/Ji
Grande
% relative to euchromatin
400
350
300
250
200
150
100
50
0
-50
Cents.
Knobs
TR-1
DNA
Retro
SD

FIGURE 3.6: Patterns of retroelement staining at knobs. Enlargements of knobs from the cells shown in figure 3.3, although some are from different optical sections. (A) Image of DNA showing intensely-staining heterochromatic knobs. (B) Same image showing only the FITC (retroelement) staining. Note that *Huck* staining at the knob is markedly reduced.

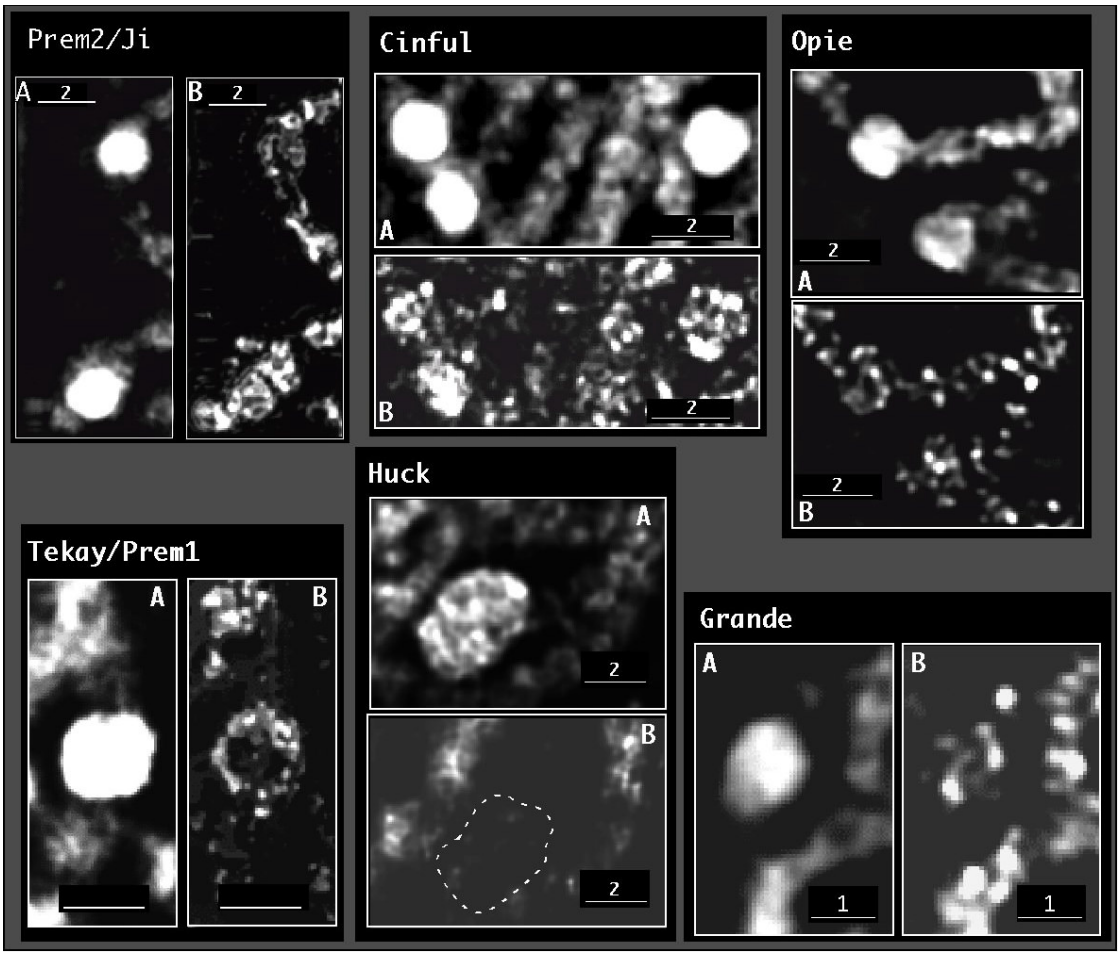
Prem2/Ji
A
2
B
2
Cinful
A
2
B
2
Opie
2
A
2
B
Huck
A
2
B
2
Tekay/Prem1
A
B
Grande
A
1
B
1

FIGURE 3.7: Staining patterns of the maize CR elements. For each panel the name of the retroelement is indicated. The DNA is shown in blue, the retroelement is shown in red and the centromeric repeat CentC is shown in green. Large images are single optical sections from maize pachytene cells. (A) 3X enlargement of the boxed regions. (B) Same images as A except only CentC staining is shown. (C) Same images as A showing only the retroelement staining.

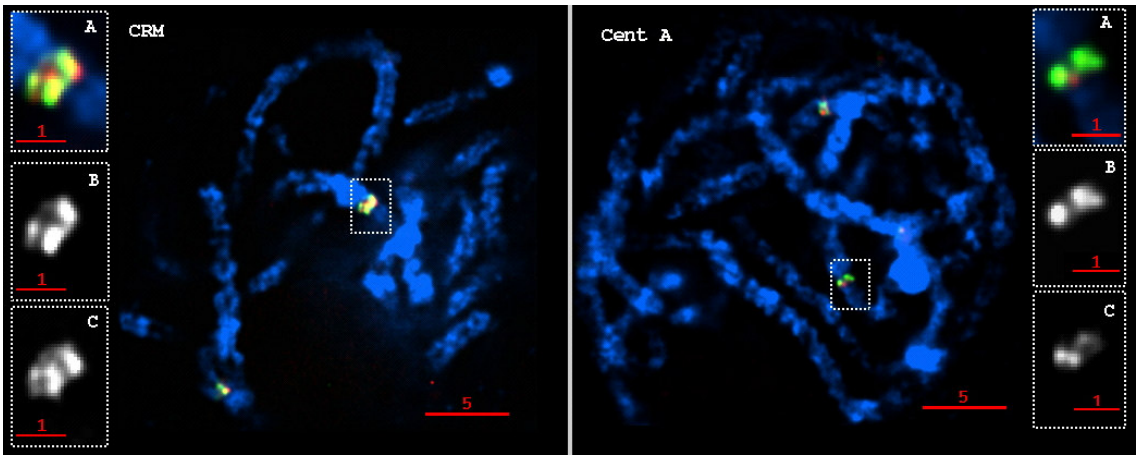
A
1
B
1
C
1
CRM
5
Cent A
5
A
1
B
1
C
1

CHAPTER 4

DISCUSSION AND CONCLUSIONS

The Ab10 chromosome of maize maintains a meiotic drive system that causes the preferential segregation of knobs and their linked loci. In this study I sought to better understand the structure and organization of the Ab10 chromosome. In my analyses I integrated the molecular and genetic maps of the N10 chromosome and created a molecular map of Ab10 in order to investigate rearrangements known to exist on the chromosome. Cytogenetic analysis was also used to examine the distribution of transposable elements on this chromosome as well as in active satellite sequences of the maize genome.

Rearrangements of the Ab10 chromosome

Most meiotic drive systems are under the control of multiple factors that are maintained in tight linkage through numerous chromosomal rearrangements (HAMMER et al. 1991; KUSANO et al. 2003; LYTTLE 1991). Such tight linkage prevents recombination of the drive chromosome with its sensitive homologue and preserves its integrity (LYTTLE 1991). Meiotic drive results from the activities of multiple drive loci; however, a successful drive system cannot evolve without chromosomal rearrangements that tie the essential elements into a single, non-recombining unit. Without these chromosomal

rearrangements there would not be drive systems but only randomly-recombining sensitive and insensitive drive and responder loci.

The Ab10 chromosome of maize is known to have at least one inverted region (RHOADES and DEMPSEY 1985), as well as other chromosomal rearrangements that make it cytologically distinguishable from N10 (LONGLEY 1937; LONGLEY 1938). Here I have analyzed the inverted segment of Ab10 by creating a molecular map of the region. These data molecularly define the boundaries of the inversion described by Rhoades and Dempsey (1985), and reveal an additional, small inversion within the larger inversion (see FIGURE 2.5). Presented in Figure 4.1 are two models for the origin of the Ab10 chromosome through a series of chromosomal rearrangements of N10. Both models begin with the translocation of a non-N10-derived chromosomal segment onto the terminal end of N10. In the first model (FIGURE 4.1A), this segment contains the differential segment, large knob and distal tip as well as the basic functions necessary for drive. In the second rearrangement, one of two translocations occur, either the euchromatic portion of N10 containing the *W2, O7, L13* and *Sr2* loci translocates distally to a location between the three chromomeres and the large knob, or the differential segment containing the chromomeres translocates proximally to a location between the *R* and *W2* loci. Either of these translocations separates the Tr-1 neocentromere activity and Tr-1 chromomeres from the remaining drive components. The large and small inversions reported here represent rearrangements three and four of the model and serve to re-associate all drive components, creating the current Ab10 chromosome.

In the second model (FIGURE 4.1B), the translocated segment of the first rearrangement contains only the large knob and associated 180-bp neocentromere activity

and distal tip function. The second rearrangement is the insertion of a second chromosomal segment containing the Tr-1 chromomeres and associated Tr-1 mediated neocentromere activity of the differential segment into the chromosome between the *R* and *W2* loci. Following this insertion, the two models merge for rearrangements three and four which serve to anchor the newly arrived Tr-1 neocentromere activity with the other drive components.

Interestingly, the regions of the chromosome known to harbor factors involved in Ab10-mediated meiotic drive are near the breakpoints of the inversions (see FIGURE 2.2). These data suggest that the complex of inversions is serving to anchor the components of the drive system together. The distal tip function, also required for meiotic drive is maintained in the small euchromatic tip, immediately adjacent to the large heterochromatic knob. The knob would be expected to suppress recombination in surrounding DNA, as well as distal tip. A picture of the organization of the Ab10 chromosome emerges involving a complex of drive loci intermingled with knobs; the ultimate targets of meiotic drive. The nested inversions, and presence and location of the knobs serve to maintain all components of the Ab10 drive system as one, preferentially segregating unit.

The most severe deficiency examined in this report Df-C, which has a breakpoint just distal to the end of the differential segment. Because of the location of this breakpoint, it is unknown if those RFLPs located proximal to the Df-C breakpoint are located in the small piece of euchromatin maintained on Df-C, or if they are located in the euchromatin located between the *R* locus and the differential segment. More recently a more severe deficiency of Ab10, Df-B, was identified (HIATT and DAWE 2003b). Df-B

has a breakpoint in the third chromomere of the differential segment (HIATT and DAWE 2003b). Analysis of the proximally located RFLPs using this chromosome would help to further define the proximal region of the Ab10 chromosome. Additionally, analysis of any RFLP markers found on the N10 chromosome that are located distal to csu48/dba3 would help to better define the small inversion on N10.

Distribution of retroelements in centromeres and neocentromeres of maize

It is known that the centromeric satellite repeat of maize, CentC, is interrupted by two centromere-specific retroelement families (CRs) CentA and CRM, and all have been found to interact with the kinetochore protein CENH3 (ANANIEV et al. 1998a; JIANG et al. 1996; ZHONG et al. 2002). Like centromeres, maize knobs, which act as neocentromeres in the presence of Ab10, are primarily composed of satellite repeats interspersed with retroelements (ANANIEV et al. 1998b; ANANIEV et al. 1998c; DENNIS and PEACOCK 1984; PEACOCK et al. 1981). However, the extent to which the most abundant retroelements in maize occupy centromeres and neocentromeres was not known prior to my study (FESCHOTTE et al. 2002a).

Using in situ hybridization I found that the major retroelement families in maize are present at significantly reduced levels in centromeric DNA. As discussed in Chapters 1 and 3, the satellite DNA of the centromere must maintain a proper structural organization to ensure continued interaction with kinetochore proteins. The CRs present at maize centromeres have been shown to interact with CENH3, indicative of their having a probable role in proper centromere function (ZHONG et al. 2002). Non-CR retroelement families, however, do not interact with CENH3, and their insertion into the centromeric

DNA could result in a reorganization of the centromeric DNA structure, preventing proper function.

Given the capacity of Ab10 to preferentially segregate to progeny, we wondered whether the Ab10 chromosome and neocentromeres would be unusually favorable niches for the insertion and accumulation of transposable elements. The experimental results presented in Chapter 3, however, show that neither Ab10 nor the neocentromeres appear to be accumulating retroelements. Evolutionarily speaking, the Ab10 chromosome and the drive system it harbors are quite young, ~500,000 years old (Buckler, personal communication). Therefore it remains possible that it is selectively advantageous for transposable elements to accumulate in the meiotic drive system, but that insufficient time has elapsed to observe it.

One interesting outcome of the analyses, however, was that knobs show a slight reduction in retroelement accumulation. Our current model is that neocentromeres, like centromeres, must maintain a proper organization of satellite DNA to retain their ability to interact with neocentromere-activating proteins. Because of the requirement for knob satellite repeats to function when the Ab10 chromosome is present, knobs may not accumulate retroelements in order to maintain their ability to act as neocentromeres when required. Under this model retroelements interfere with the organization of knob chromatin and are selectively disadvantageous to the drive system.

Composition of the Ab10 chromosome

The Ab10 chromosome of maize contains a significant amount of additional chromatin as compared to the N10 chromosome: in fact, there is approximately as much

additional chromatin on Ab10 as in the entire small arm of the N10 chromosome (LONGLEY 1937; LONGLEY 1938; RHOADES 1942). Where did all this DNA come from? Recently, Hiatt and Dawe (2003) have shown that there are few essential genes located in the additional chromatin present on Ab10, suggesting that much of the DNA is repetitive or non-essential. However, my data suggest that neither LTR retroelements nor MITEs are accumulating on Ab10. The possibility remains that other, uncharacterized transposable elements are abundant on this chromosome. An alternative scenario is that much of the chromatin on Ab10 is low copy or genic DNA, and that it is simply an unusually redundant portion of the genome. Maize genome sequencing efforts currently underway may help to resolve this issue.

Figure 4.1: Two models for the creation of Ab10 from N10. A. The first model begins with the translocation of the differential segment, large knob and distal tip and associated functions onto the distal end of N10. Rearrangement 2 involves one of the two translocations that are diagrammed. B. The second model begins with the translocation of the large knob and distal tip with associated functions onto the terminal end of N10. The second rearrangement is the insertion of the differential segment into the long arm of N10. The two models merge for rearrangements three and four, representing, in either order, the two inversions described in Chapter 2.

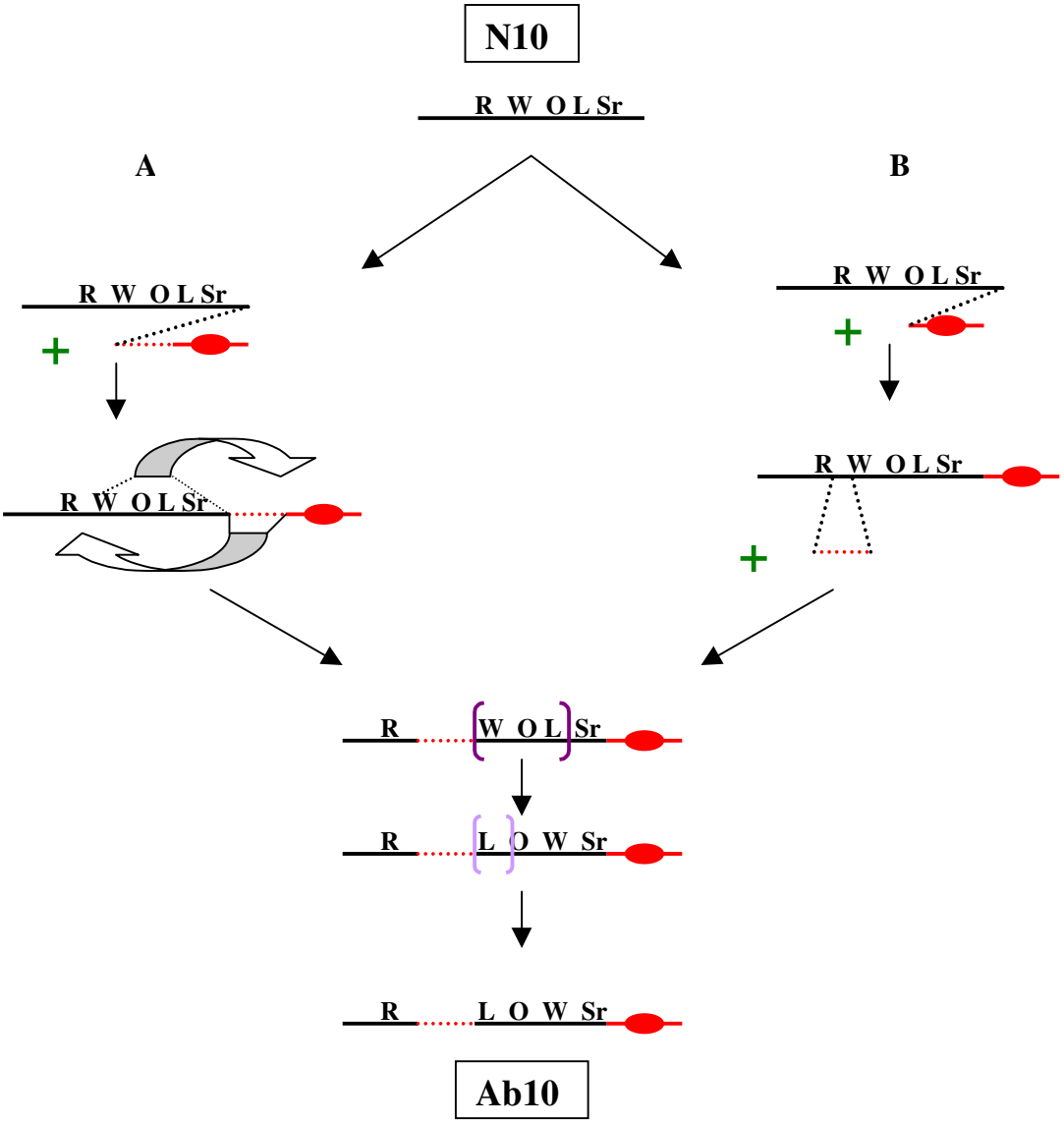
N10
R W O L Sr
A
B
R W O L Sr
+
R W O L Sr
R W O L Sr
+
R W O L Sr
R W O L Sr
R W O L Sr
R L O W Sr
R L O W Sr
Ab10

APPENDIX

TRANSPOSON DISPLAY ANALYSIS OF MITES IN THE DISTAL TIP OF THE AB10 CHROMOSOME OF MAIZE

Introduction

Transposable elements are mobile units of a genome and often make up a majority of the genome in which they reside (BENNETZEN 2002; BENNETZEN et al. 1998; FESCHOTTE et al. 2002a). Transposable elements are separated into two major classes. Class I elements are called retroelements, and move via an RNA intermediate that is reverse transcribed into DNA. Class II, or DNA elements move through excision of the original, double stranded DNA element and reinsertion elsewhere in the genome, and are bound by terminal inverted repeats (TIRs).

Class II elements are either autonomous or non autonomous. Virtually all class II elements terminate with inverted repeats called terminal inverted repeats (TIR). Autonomous elements encode transposase and all other proteins necessary for their transposition. Non-autonomous elements have maintained the cis-sequences necessary for recognition by transposase, but are unable to promote their own movement because they do not encode transposase. Non-autonomous elements can be mobilized only when there is an autonomous element in the genome producing transposase that facilitates their movement.

In maize an many other organisms, their exists a group of Class II elements called miniature inverted repeat transposable elements (MITEs) (BUREAU and WESSLER 1992; BUREAU and WESSLER 1994; FESCHOTTE et al. 2002a; FESCHOTTE et al. 2002b). MITEs are non-autonomous elements, having TIRs of 10-30 bp in length. Unlike most other non autonomous elements that have been described, MITEs are very small, only 100-500 bp in total length, and can attain extremely high copy numbers in a variety of species (BUREAU and WESSLER 1992; BUREAU and WESSLER 1994; CASA et al. 2000; FESCHOTTE et al. 2002b). MITEs, like most class II elements, have also been shown to have a preference for inserting into genes (FESCHOTTE et al. 2002a; FESCHOTTE et al. 2002b).

The Heartbreaker (*Hbr*) MITE family in maize, unlike many previously described MITEs, has extremely high TIR sequence identity (over 90%) among its family members (ZHANG et al. 2000). *Hbr* family members also show a high degree of polymorphism in insertion sites when maize strains are compared (CASA et al. 2000; ZHANG et al. 2000). Because of these characteristics of the *Hbr* MITE family, a modification of the AFLP technique was developed, called transposon display (TD), as a method for using *Hbr* insertion sites as a new type of molecular marker in maize (CASA et al. 2000). Analysis of *Hbr* elements by TD has shown that they are evenly distributed throughout the genome (CASA et al. 2000). Transposon display has also been successfully developed the MITE family *mPIF* (X. Zhang and S.R. Wessler, unpublished data).

In maize there exists an unusual chromosome called Abnormal chromosome 10 (Ab10). The Ab10 chromosome is an aberrant form of the normal 10 (N10) chromosome that is cytologically distinguishable from its N10 homologue (LONGLEY 1937; LONGLEY 1938). Ab10 can be identified by the additional chromatin present on the distal portion of

the chromosome's long arm (see FIGURE 1.1). This chromatin is composed of four regions: the differential segment containing three small chromomeres, the inverted region that is homologous to a portion of N10, a large heterochromatic knob, and a small euchromatic distal tip of unknown origin (LONGLEY 1937; LONGLEY 1938; RHOADES 1942; RHOADES and DEMPSEY 1985) (see FIGURE 1.1). Presence of this chromosome in the genome results in the preferential segregation and neocentromere activity of knobs, and also increases recombination frequencies in certain regions of the genome (LONGLEY 1945; RHOADES 1942; RHOADES 1950; RHOADES 1952; RHOADES and DEMPSEY 1957; RHOADES and DEMPSEY 1966; RHOADES and DEMPSEY 1985).

A deficiency of the Ab10 chromosome has been recovered that has lost the distal euchromatic tip (Deficiency-L or Df-L), as well as its ability to cause preferential segregation (HIATT and DAWE 2003a) (see FIGURE 1.3). This function is referred to as the distal tip function (HIATT and DAWE 2003a). Because of their use as molecular markers, and their association with genes in maize we used TD analysis of the *Hbr* and *mPIF* MITE families to examine the Ab10 chromosome. TD results in PCR products containing one end of a MITE along with flanking DNA, potentially belonging to a gene. TD was used to locate MITEs in the distal tip with the hope that we might uncover a gene(s) located on Df-L potentially involved in meiotic drive. Here I describe the identification of two Df-L specific MITEs.

Materials and Methods

Plant material

The Ab10 and Df-C seed stocks were originally obtained by R. K. Dawe from M. Rhoades and subsequently back crossed into the *W23* background five times. Df-L was discovered by R. K. Dawe and also back crossed into the *W23* background five times. Ten kernels were germinated for each Ab10, Df-C, and Df-L genotype. Ten N10 full-sib kernels for each deficiency were also germinated and analyzed in each experiment to serve as controls. DNA was isolated from each of the ten plants and pooled to control for background polymorphism.

Transposon Display

For each of the genotypes being examined, 200-500 ng of DNA were digested with either *Mse*I or *Bfa*I and adapters were ligated to the digested ends as described (CASA et al. 2000). Upon the addition of adapter sequences, these digestion/ligation reactions were used for all TD analyses. Both *Mse*I and *Bfa*I digestion/ligation reactions were used in the *Hbr* analysis. Due to an *Mse*I site in the *mPIF* element, only the *Bfa*I digestion/ligation reaction was used in *mPIF* TD analysis.

For *Hbr* TD analysis pre-selective and selective amplifications were carried out using the primers and PCR reactions and cycling parameters described (CASA et al. 2000). For *mPIF* TD, only the *Bfa*I digestion/ligation reaction was used in the pre-selective amplification, which was performed as described by Casa et al. (2000), substituting the *mPIF* primer, (PI-73: 5' -TGGAAAGTGGTGGAATGTC-3') for the *Hbr* pre-selective primer. The selective amplification reactions were carried out as described by Casa et al (2000) using the *Bfa*I primer with one selective base and substituting ^{33}P-labeled *mPIF* primer, (PI20L: 5' -ASTWAGATTCCAATTCCTCAAAATGAA-3') for

the *Hbr* selective primer. All selective amplification reactions for each MITE family were electrophoresed and examined as described for radioactive visualization of bands (CASA et al. 2000).

Recovery and re-amplification of bands

TD bands of interest were excised from the acrylamide gels and used as templates for PCR. PCR reactions were prepared using the same selective amplification primer pairs that originally generated the fragment, and temperature cycling was performed as was done for the original selective amplification. Purified fragments were cloned using the TOPO-TA cloning kit (Invitrogen, Carlsbad, CA) and multiple clones from each reaction were sequenced. Fragment sequences were aligned to each other using MacVector (Accelrys Inc., San Diego, CA), and DNA sequences flanking the MITE were identified. Flanking DNA sequences were used as queries in BLAST searches to determine the nature of the flanking DNA sequences.

Results

TD was performed for both MITE families in order to identify MITE insertions specific to the distal tip of the Ab10 chromosome. In order to accomplish this, MITE display was performed using Ab10, a large deletion of Ab10 known as Df-C, and Df-L (see FIGURE 1.3). N10 sibs of each chromosome were analyzed in parallel with the Ab10 genotypes. TD bands were considered to be located in the distal tip if the band was present in Ab10 and missing from the Df-C, Df-L, and all N10 lanes.

Because of an *Mse*I site in the *mPIF* sequence, only the *Bfa*I+ one selective base primer combinations were used in TD analysis of the *mPIF* MITE family. These four reactions produced one band (*mPIF-Bfa*I+G) that was potentially specific to the distal tip (FIGURE A.1A) This band proved highly resistant to re-amplification and cloning, and was not further analyzed.

For the *Hbr* MITE family, TD analysis was carried out using *Mse*I and *Bfa*I amplifications with one selective base, for a total of 8 primer combinations examined. From these reactions only the *Mse*I+C and *Mse*I+G primers produced a single band potentially specific to the distal tip (FIGURE A.1B). The *Mse*I+G band was re-amplified, cloned and sequenced. A BLAST search revealed that the DNA flanking this particular element was part of Grande-1, an abundant retroelement family (SANMIGUEL and BENNETZEN 1998).

Discussion

TD is a modification of the AFLP technique that is used to analyze transposable element (TE) insertions in genomic DNA. Using one primer anchored at an enzyme restriction site (*Mse*I or *Bfa*I) and another primer anchored adjacent to the TIR of a particular TE, PCR fragments are generated that can be used as molecular markers. The TD protocol allows for analysis of DNA sequences flanking the TE being examined through excision of the PCR band from the TD gel. Given the genic preference of MITEs it was hoped that the TD protocol could be used to identify genes on Ab10. Here we have used TD analysis in an attempt to identify MITEs located in the distal tip of Ab10.

In the analysis of *Hbr* undertaken by Casa et al. (2002), 252 polymorphic bands were mapped throughout the maize genome. Since the distal tip of Ab10 represents approximately 0.6% of the genome, it would be expected to harbor roughly 1-2 *Hbr* TD bands. In my studies I was able to identify two polymorphic bands, suggesting that the distal tip is similar in constitution to other regions of the genome.

In total there are approximately 4,000 *Hbr* elements in the maize genome (ZHANG et al. 2000), and the *mPIF* family of MITEs has approximately 6,000 members in maize (ZHANG et al. 2001). It was expected that the distal tip would produce 2-3 *mPIF* bands using TD. Although the single band found on the distal tip is not significantly different than expected, this family may be under represented in this region of the maize genome.

The fact that the two MITEs found in the distal tip were not inserted into genes was unexpected given the genic preference of MITEs. It has recently been revealed, however, that the entire distal region of Ab10 contains few genes (HIATT and DAWE 2003b). This finding may explain why the two identified sequences were not part of genes. It remains possible that fragments I was unable to clone represent MITE associations with genes on the distal tip of Ab10. The Ab10 chromosome is a preferentially segregating chromosome contributing, apparently, no benefit to its host. This analysis has shown that although both the Ab10 chromosome and transposable elements are selfish elements, the MITE families examined here did not show a significant increase in accumulation in this chromosome. Although the MITE families examined here have not accumulated extensively on Ab10, it is possible that Ab10 formed after these MITE families stopped transposing, and that other, more recently active MITEs may show accumulation on Ab10.

FIGURE A.1: Autoradiographs of transposon display analysis of maize genomic DNA with MITE primers. Genotypes are labeled at the top of each lane. Marker: 30-300bp ladder; Ab10: heterozygous Ab10; N10/A: N10 full-sibs of the Ab10 genotype; Df-C: heterozygous Df-C; N10/C: N10 full-sibs of the Df-C genotype; Df-L: heterozygous Df-L; N10/L: N10 full-sibs of the Df-L genotype. A. mPIF-BfaI+G transposon display reaction. B. Hbr-MseI+C and Hbr-MseI+G transposon display reactions. All distal-tip-specific band candidates indicated by red arrows.

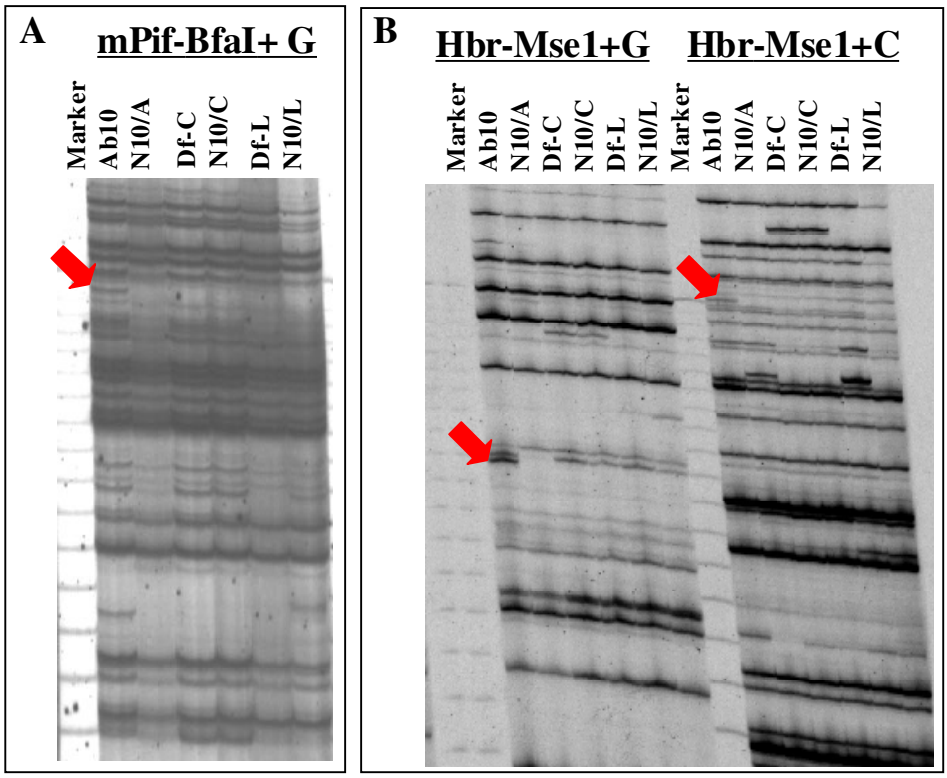
A
mPif-BfaI+ G
Marker
Ab10
N10/A
Df-C
N10/C
Df-L
N10/L
B
Hbr-Mse1+G
Hbr-Mse1+C
Marker
Ab10
N10/A
Df-C
N10/C
Df-L
N10/L
Marker
Ab10
N10/A
Df-C
N10/C
Df-L
N10/L

REFERENCES

AMOR, J. D., and K. H. A. CHOO, 2002 Neocentromeres: role in human disease, evolution, and centromere study. Am. J. Hum. Genet. **71:** 695-714.

ANANIEV, E. V., R. L. PHILLIPS and H. W. RINES, 1998a Chromosome-specific molecular organization of maize (*Zea mays* L.) centromeric regions. Proceedings of The National Academy of Sciences **95:** 13073-13078.

ANANIEV, E. V., R. L. PHILLIPS and H. W. RINES, 1998b Complex structure of knob DNA on maize chromosome 9: retrotransposon invasion into heterochromatin. Genetics **149:** 2025-2037.

ANANIEV, E. V., R. L. PHILLIPS and H. W. RINES, 1998c A knob-associated tandem repeat in maize capable of forming fold-back DNA segments: Are chromosome knobs megatransposons? Proceedings of The National Academy of Sciences **95:** 10785-10790.

ARAGON-ALCAIDE, L., T. MILLER, T. SCHWARZACHER, S. READER and G. MOORE, 1996 A cereal centromeric sequence. Chromosoma **105:** 261-268.

ARDLIE, K. G., 1998 Putting the brake on drive: meiotic drive of t-haplotypes in natural populations of mice. Trends in Genetics **14:** 189-193.

BEADLE, G. W., and A. H. STURTEVANT, 1935 X chromosome inversions and meiosis in Drosophila melanogaster. Proc. Natl. Acad. Sci. **21:** 384-390.

BENNETZEN, J. L., 2002 Mechanisms and rates of genome expansion and contraction in flowering plants. Genetica **115:** 29-36.

BENNETZEN, J. L., P. SANMIGUEL, M. CHEN, A. TIKHONOV, M. FRANCKI et al., 1998 Grass Genomes. Proceedings of The National Academy of Sciences **95:** 1975-1978.

BOWEN, N., and J. F. MCDONALD, 2001 Drosophila euchromatic LTR retrotransposons are much younger than the host species in which they reside. Genome Research **11:** 1527-1540.

BRANDES, A., J. S. HESLOP-HARRISON, A. KAMM, S. KUBIS, R. L. DOUDRICK et al., 1997 Comparative analysis of the chromosomal and genomic organization of *Ty*1-*copia*-like retrotransposons in pteridophytes, gymnosperms and angiosperms. Plant Molecular Biology **33:** 11-21.

BUCKLER, E. S. I., T. L. PHELPS-DURR, C. S. KEITH BUCKLER, R. K. DAWE, J. F. DOEBLEY et al., 1999 Meiotic drive of knobs reshaped the maize genome. Genetics **153:** 415-426.

BUREAU, T. E., and S. R. WESSLER, 1992 Tourist: a large family of small inverted repeat elements frequently associated with maize genes. Plant Cell **4:** 1283-1294.

BUREAU, T. E., and S. R. WESSLER, 1994 Mobile inverted-repeat elements of the tourist family are associated with the genes of many cereal grasses. Proc. Natl. Acad. Sci. **91:** 1411-1415.

CARLSON, W. R., 1977 The Cytogenetics of Corn, pp. 225-304 in *Corn and corn improvement*, edited by G. F. Sprague. American Society of Agronomy, Inc., Madison, Wisconsin.

CASA, A. M., C. BROUWER, A. NAGEL, L. WANG, Q. ZHANG et al., 2000 The MITE family Heartvreaker (Hbr): molecular markers in maize. Proc. Natl. Acad. Sci. **97:** 10083-10090.

CASACUBERTA, E., and M. L. PARDU, 2003 Transposon telomeres are widely distributed in the *Drosophila* genus: TART elements in the *virilis* group. Proc. Natl. Acad. Sci. **100:** 3363-3368.

CAVALIER-SMITH, T., 1978 Nuclear volume control by nucleoskeletal DNA, selection for cell volume and cell growth rate, and the solution of the DNA C-value paradox. Journal of Cell Science **34:** 247-278.

CHENG, Z., F. DONG, T. LANGDON, S. OUYANG, C. R. BUELL et al., 2002 Functional rice centromeres are marked by a satellite repeat and a centromere-specific retrotransposon. Plant Cell **14:** 1691-1704.

CHOO, K. H. A., 2001 Domain organization at the centromere and neocentromere. Cell **1:** 165-177.

DAWE, R. K., and W. Z. CANDE, 1996 Induction of centromeric activity in maize by suppressor of meiotic drive 1. Proceedings of The National Academy of Sciences **93:** 8512-8517.

DAWE, R. K., L. S. REED, H. G. YU, M. G. MUSZYNSKI and E. N. HIATT, 1999 A maize homolog of mammalian CENPC is a constitutive component of the inner kinetochore. Plant Cell **11:** 1227-1238.

DAWE, R. K., J. W. SEDAT, D. A. AGARD and W. Z. CANDE, 1994 Meiotic chromosome pairing in maize is associated with novel chromatin organization. Cell **76:** 901-912.

DENNIS, E. S., and W. J. PEACOCK, 1984 Knob heterochromatin homology in maize and its relatives. Journal of Molecular Evolution **20:** 341-350.

EDWARDS, K. J., J. VEUSKENS, H. RAWLES, A. DALY and J. L. BENNETZEN, 1996 Characterization of four dispersed repetitive DNA sequences from *Zea mays* and their use in constructing contiguous DNA fragments using YAC clones. Genome **39:** 811-817.

EICKBUSH, T. H., 2002 R2 and related site-specific non-long terminal repeat retrotransposons, pp. 813-835 in *Mobile DNA II*, edited by N. L. e. a. Craig. ASM Press, Washington D.C.

EMMERLING, M. H., 1959 Preferential segregation of structurally modified chromosomes in maize. Genetics **44:** 625-645.

FENG, D. F., and R. F. DOOLITTLE, 1987 Progressive sequence alignment as a prerequisite to correct phylogenetic trees. Journal of Molecular Evolution **25:** 351-360.

FENG, Q., Y. ZHANG, P. HAO, S. WANG and G. FU, 2002 Sequence and analysis of rice chromosome 4. Nature **420:** 316-320.

FESCHOTTE, C., N. JIANG and S. R. WESSLER, 2002a Plant transposable elements: where genetics meets genomics. Nature Reviews Genetics **3:** 329-341.

FESCHOTTE, C., X. ZHANG and S. R. WESSLER, 2002b Miniature inverted-repeat transposable elements and their relationship to established DNA transposons, pp.

1147-1158 in *Mobile DNA II*, edited by N. L. Craig, R. Craigie, M. Gellert and A. Lambowitz. ASM Press, Washington, D.C.

FRIESEN, N., A. BRANDES and J. S. HESLOP-HARRISON, 2001 Diversity, Origin, and Distribution of Retrotransposons (*gypsy* and *copia*) in Conifers. Molecular Biology and Evolution **18:** 1176-1188.

GCG, 1982-2000 Wisconsin package, pp. Genetics Computer Group, Inc., Madison.

GRIMES, B. R., A. A. RHOADES and H. F. WILLARD, 2002 Alpha-satellite DNA and vector composition influence rates of human artificial chromosome formation. Mol Ther. **5:** 798-805.

HAMMER, M. F., S. BLISS and L. M. SILVER, 1991 Genetic exchange across a paracentric inversion of the Mouse t complex. Genetics **128:** 799-812.

HAUPT, W., T. C. FISCHER, S. WINDERL, P. FRANSZ and R. A. TORRES-RUIZ, 2001 The centromere 1 (CEN1) region of *Arabidopsis thaliana*: architecture and functional impact of chromatin. Plant J. **27:** 285-296.

HENIKOFF, S., 2002 Near the edge of a chromosome' s "black hole". Trends in Genetics **18:** 165-167.

HENIKOFF, S., K. AHMAD and H. S. MALIK, 2001 The centromere paradox: stable inheritance with rapidly evolving DNA. Science **293:** 1098-1102.

HENIKOFF, S., and J. G. HENIKOFF, 1992 Amino acid substitution matrices from protein blocks. Proceedings of The National Academy of Sciences **89:** 10915-10919.

HESLOP-HARRISON, J. S., A. BRANDES and T. SCHWARZACHER, 2003 Tandemly repeated DNA sequences and centromeric chromosomal regions of *Arabidopsis* species. Chromosome Research **11:** 241-253.

HIATT, E. N., and R. K. DAWE, 2003a Four loci on Abnormal chromosome 10 contribute to meiotic drive in maize. Genetics **In Press**.

HIATT, E. N., and R. K. DAWE, 2003b The meiotic drive system on maize abnormal chromosome 10 contains few essential genes. Genetica **117:** 67-76.

HIATT, E. N., E. K. KENTNER and R. K. DAWE, 2002 Independently regulated neocentromere activity of two classes of tandem repeat arrays. The Plant Cell **14:** 407-420.

HOSOUCHI, T., N. KUMEKAWA, H. TSURUOKA and H. KOTANI, 2002 Physical map-based sized of the centromeric regions of *Arabidopsis thaliana* chromosomes 1,2, and 3. DNA Res. **9:** 117-121.

HOUTCHENS, K., and T. W. LYTTLE, 2003 Responder (Rsp) alleles in the segregation distorter (SD) system of meiotic drive in Drosophila may represent a complex family of satellite repeat sequences. Genetica **117:** 291-302.

HUDAKOVA, S., W. MICHALEK, G. G. PRESTING, R. TEN HOOPEN, K. DOS SANTOS et al., 2001 Sequence organization of barley centromeres. Nucleic Acids Research **29:** 5029-5035.

INITIATIVE, A. G., 2000 Analysis of the genome sequence of the flowering plant *Arabidopsis thaliana*. Nature **408:** 796-815.

JIANG, J., A. NASUDA, F. DONG, C. SCHERRER, S. S. WOO et al., 1996 A conserved repetitive DNA element located in the centromeres of cereal

chromosomes. Proceedings of The National Academy of Sciences **93:** 14210-14213.

KATO, Y. T. A., 1976 Cytological studies of maize (*Zea mays* L.) and teosinte (*Zea mexicana*) in relation to their origin and evolution. Massachusetts Agricultural Experiment Station Bulletin **635:** 1-185.

KERMICLE, J. L., and J. D. AXTELL, 1981 Modification of chlorophyll striping by the *R* region. Maydica **26:** 197.

KIKUDOME, G. Y., 1959 Studies on the phenomenon of preferential segregation in maize. Genetics **44:** 815-831.

KOZIK, A., E. KOCHETKOVA and R. MICHELMORE, 2002 GenomePixelizer: a visualization program for comparative genomics within and between species. Bioinformatics **18:** 335-336.

KUMAR, A., and J. L. BENNETZEN, 1999 Plant Retrotransposons. Annual Review of Genetics **33:** 479-532.

KUMAR, A., S. R. PEARCE, K. MCLEAN, G. HARRISON, J. S. HESLOP-HARRISON et al., 1997 The Ty1-*copia* group of retrotransposons in plants: genomic organisation, evolution, and use as molecular markers. Genetica **100:** 205-217.

KUMEKAWA, N., T. HOSOUCHI, H. TSURUOKA and H. KOTANI, 2000 The size and sequence organization of the centromeric region of *Arabidopsis thaliana* chromosome 5. DNA Res **7:** 315-321.

KUMEKAWA, N., T. HOSOUCHI, H. TSURUOKA and H. KOTANI, 2001 The size and sequence organization of the centromeric region of Arabidopsis thaliana chromosome 4. DNA Research **8:** 285-290.

KUSANO, A., C. STABER and H. Y. E. CHAN, 2003 Closing the (Ran)GAP on segregation distortion in *Drosophila*. BioEssays **25:** 108-115.

LANDER, E. S., P. GREEN, J. ABRAHAMSON, A. BARLOW, M. J. DALY et al., 1987 MAPMAKER: an interactive computer package for constructing primary genetic linkage maps of experimental and natural populations. Genomics **1:** 174-181.

LANGDON, T., C. SEAGO, M. MENDE, M. LEGGETT, H. THOMAS et al., 2000 Retrotransposon Evolution in Diverse Plant Genomes. Genetics **156:** 313-325.

LONGLEY, A. E., 1937 Morphological characters of teosinte chromosomes. J. Agric. Res. **59:** 475-490.

LONGLEY, A. E., 1938 Chromosomes of maize from North American Indians. J. Agric. Res. **56:** 177-195.

LONGLEY, A. E., 1945 Abnormal segregation during megasporogenesis in maize. Genetics **30:** 100-113.

LYTTLE, T. W., 1991 Segregation distorters. Annu. Rev. Genet. **25:** 511-557.

LYTTLE, T. W., 1993 Cheaters sometimes prosper: distortion of mendelian segregation by meiotic drive. Trends Genet. **9:** 205-210.

MALIK, H. S., and T. H. EICKBUSH, 1999 Modular Evolution of the Integrase Domain in the Ty3/Gypsy Class of LTR Retrotransposons. Journal of Virology **73:** 5186-5190.

MALIK, H. S., and S. HENIKOFF, 2001 Adaptive evolution of Cid, a centromere-specific histone in drosophila. Genetics **157:** 1293-1298.

MERRILL, C., L. BAYRAKTAROGLU, A. KUSANO and B. GANETZKY, 1999 Truncated RanGAP encoded by the Segregation Distorter locus of Drosophila. Science **283:** 1742-1745.

MEYERS, B. C., S. V. TINGEY and M. MORGANTE, 2001 Abundance, Distribution, and Transcriptional Activity of Repetitive Elements in the Maize Genome. Genome Research **11:** 1660-1676.

MILES, J. H., 1970 Influence of modified K10 chromosomes on prefernetial segregation and crossing over in Zea mays., pp. Indiana University, Bloomington, Indiana.

MILLER, J. T., F. DONG, S. A. JACKSON, J. SONG and J. JIANG, 1998 Retrotransposon-related DNA sequences in the centromeres of grass chromosomes. Genetics **150:** 1615-1623.

MROCZEK, R., and R. K. DAWE, 2003 Distributionof retroelements in centromeres and neocentromeres of maize. Genetics **Accepted pending revisions**.

NAGAKI, K., J. SONG, R. M. STUPAR, A. S. PAROKONNY, Q. YUAN et al., 2003a Molecular and cytological analyses of large tracks of centromeric DNA reveals the structure and evolutionary dynamics of maize centromeres. Genetics **163:** 759-770.

NAGAKI, K., P. B. TALBERT, C. X. ZHONG, R. K. DAWE, S. HENIKOFF et al., 2003b Chromatin immunoprecipitation reveals that the 180-bp satellite repeat is the key functional DNA element of *Arabidopsis thaliana* centromeres. Genetics **163:** 1221-1225.

OSTERGREN, G., 1945 Parasitic nature of extra fragment chromosomes. Bot. Notiser **2:** 157-163.

PAGEL, M., and R. A. JOHNSTONE, 1992 Variation across species in the size of teh nuclear genome supports the junk-DNA explanation for the C-value paradox. Proceedings of The Royal Society of London. Series B, Biological Sciences. **249:** 119-124.

PARDU, M. L., and P. G. DEBARYSHE, 2000 Drosophila telomere transposons: genetically active elements in heterochromatin. Genetica **109:** 45-52.

PARK, S. H., H. G. CHIN, M. J. CHO, R. A. MARTIENSSEN and C. HAN, 2000 Inhibitor of striate conditionally suppresses cell proliferation in variegated maize. Genes Dev. **14:** 1005-16.

PATEL-KING, R., S. E. BENASHSKI, A. HARRISON and S. M. KING, 1997 A Chlamydomonas homologue of the putative murine t complex distorter Tctex-2 is an outer arm dynein light chain. J. Cell Biol. **137:** 1081-1090.

PEACOCK, W. J., E. S. DENNIS, M. M. RHOADES and A. J. PRYOR, 1981 Highly repeated DNA sequence limited to knob heterochromatin in maize. Proceedings of The National Academy of Sciences **78:** 4490-4494.

PEARCE, S. R., G. HARRISON, J. S. HESLOP-HARRISON, A. J. FLAVELL and A. KUMAR, 1997 Characterisation and genomic organisation of Ty1-*copia* group retrotransposons in rye (*Secale cereale*). Genome **40:** 617-25.

PEARCE, S. R., G. HARRISON, D. LI, J. S. HESLOP-HARRISON, A. KUMAR et al., 1996a The *Ty1-copia* group retrotransposons in *Vicia* species: copy number,

sequence heterogeneity and chromosomal localisation. Mol Gen Genet **250:** 305-315.

PEARCE, S. R., U. PICH, G. HARRISON, A. J. FLAVELL and J. S. HESLOP-HARRISON, 1996b The Ty1-copia group retrotransposons of Allium cepa are distributed throughout the chromosomes but are enriched in the terminal heterochromatin. Chromosome Research **4:** 357-364.

PEREZ-GONZALEZ, C., and T. H. EICHBUSH, 2002 Rates of R1 and R2 retrotransposition and elimination from the rDNA locus of Drosophila melanogaster. Genetics **162:** 799-811.

PICH, U., and I. SCHUBERT, 1998 Terminal heterochromatin and alternative telomeric sequences in Allium cepa. Chromosome Res. **6:** 315-321.

PRESTING, G. G., L. MALYSHEVA, J. FUCHS and I. SCHUBERT, 1998 A Ty3/Gypsy retrotransposon-like sequence localizes to the centromeric regions of cereal chromosomes. The Plant Journal **16:** 721-728.

REDKAR, A. A., Y. SI, S. N. TWINE, S. H. PILDER and P. OLDS-CLARKE, 2000 Genes in the first and fourth inversions of the mouse t comples synergistically mediate sperm capacitation and interactions with the oocyte. Dev. Biol. **226:** 267-280.

RHOADES, M. M., 1942 Preferential segregation in maize. Genetics **27:** 395-407.

RHOADES, M. M., 1950 Meiosis in maize. Journal of Heredity **41:** 59-67.

RHOADES, M. M., 1952 Preferential segregation in maize, pp. 66-80 in *Heterosis*, edited by J. W. Gowen. Iowa State College Press, Ames, IA.

RHOADES, M. M., and E. DEMPSEY, 1953 Cytogenetic studies of deficient-duplicate chromosomes derived from inversion heterozygotes in maize. J. Bot. **40:** 405-424.

RHOADES, M. M., and E. DEMPSEY, 1957 Further studies on preferential segregation. Maize Genetics Cooperation Newsletter **31:** 77-80.

RHOADES, M. M., and E. DEMPSEY, 1966 The effect of abnormal chromosome 10 on preferential segregation and crossing over in maize. Genetics **53:** 989-1020.

RHOADES, M. M., and E. DEMPSEY, 1972 On the mechanism of chromatin loss induced by the B chromosome of maize. Genetics **71:** 73-96.

RHOADES, M. M., and E. DEMPSEY, 1985 Structural heterogeneity of chromosome 10 in races of maize and teosinte, pp. 1-18 in *Plant Genetics*, edited by M. Freeling. Alan R. Liss, New York.

RHOADES, M. M., and H. VILKOMERSON, 1942 On the anaphase movement of chromosomes. Proceedings of The National Academy of Sciences **28:** 433-436.

ROBERTSON, D., P. STINARD and M. MAGUIRE, 1994 Genetic evidence of Mutator-induced deletions in the short arm of chromosome 9 in maize. II. wd deletions. Genetics **136:** 1143-1149.

SAMANT, S. A., O. OGUNKUA, L. HUI, J. FOSSELLA and S. H. PILDER, 2002 The T complex distorter 2 candidate gene, Dnahc8, encodes at least two testis-specific axonemal dynein heavy chains that differ extensively at their amino and carboxyl termini. Dev. Biol. **25:** 24-43.

SANMIGUEL, P., and J. L. BENNETZEN, 1998 Evidence that a Recent Increase in Maize Genome Size was Caused by the Massive Amplification of Intergene Retrotransposons. Annals of Botany **82:** 37-44.

SANMIGUEL, P., B. S. GAUT, A. TIKHONOV, Y. NAKAJIMA and J. L. BENNETZEN, 1998 The Paleontology of intergene retrotransposons of maize. nature genetics **20:** 43-45.

SANMIGUEL, P., A. TIKHONOV, Y. JIN, N. MOTCHOULSKAIA, D. ZAKHAROV et al., 1996 Nested Retrotransposons in the Intergenic Regions of the Maize Genome. Science **274:** 765-768.

SCHUELER, M. G., A. W. HIGGINS, M. K. RUDD, K. GUSTASHAW and H. F. WILLARD, 2001 Genomic and genetic definition of a functional human centromere. Science **294:** 109-115.

SNIEGOWSKI, P. D., and B. CHARLESWORTH, 1994 Transposable element numbers in cosmopolitan inversions from a natural population of Drosophila melanogaster. Genetics **137:** 815-827.

SONG, J., F. DONG, J. W. LILLY, R. M. STUPAR and J. JIANG, 2001 Instability of bacterial artificial chromosome (BAC) clones containing tandemly repeated DNA sequences. Genome **44:** 463-469.

SUN, X., H. D. LEE, J. M. WAHLSTROM and G. H. KARPEN, 2003 Sequence analysis of a functional Drosophila centromere. Genome Res **13:** 182-194.

SUN, X., J. WAHLSTROM and G. KARPEN, 1997 Molecular Structure of a Functional *Drosophila* Centromere. Cell **91:** 1007-1019.

SWOFFORD, D., 1999 PAUP*, pp. Sinauer Associates, Sunderland, MA.

TIKHONOV, A. P., P. J. SANMIGUEL, Y. NAKAJIMA, N. M. GORENSTEIN, J. L. BENNETZEN et al., 1999 Colinearity and its exceptions in orthologous *adh* regions of maize and sorghum. Proceedings of The National Academy of Sciences **96:** 7409-7414.

VINCENT, C. M., A. SUONIEMI, K. ANAMTHAWAT-JONSSON, J. TANSKANEN, A. BEHARAV et al., 1999 Retrotransposon *BARE-1* and its role in genome evolution in the genus *Hordeum*. The Plant Cell **11:** 1769-1784.

WICKER, T., N. STEIN, L. ALBAR, C. FEUILLET, E. SCHLAGENHAUF et al., 2001 Analysis of a contiguous 211kb sequence in diploid wheat (Triticum monococcum L.) reveals multiple mechanisms of genome evolution. Plant Journal **26:** 307-316.

XIONG, Y., and H. EICKBUSH, 1988 Similarity of Reverse Transcriptase-like Sequences of Viruses, Transposable Elements, and Mitochondrial Introns. Mol. Biol. Evol. **5:** 675-690.

XIONG, Y., and H. EICKBUSH, 1990 Origin and evolution of retroelements based upon their reverse transcriptase sequences. The EMBO Journal **9:** 3353-3362.

YU, H. G., E. N. HIATT, A. CHAN, M. SWEENEY and R. K. DAWE, 1997 Neocentromere-mediated chromosome movement in maize. Journal of cell Biology **139:** 831-840.

ZHANG, Q., J. ARBUCKLE and S. R. WESSLER, 2000 Recent, extensive, and preferential insertion of members of the miniature inverted-repeat transposable element family *Heartbreaker* into genic regions of maize. Proc. Natl. Acad. Sci. **97:** 1160-1165.

ZHANG, X., C. FESCHOTTE, Q. ZHANG, N. JIANG, W. B. EGGLESTON et al., 2001 *P* instability factor: An active maize transposon system associated with the amplification of *Tourist*-like MITEs and a new superfamily of transposases. Proc. Natl. Acad. Sci. **98:** 12572-12577.

ZHONG, C., J. B. MARSHALL, C. TOPP, R. MROCZEK, A. KATO et al., 2002 Centromeric retroelements and satellites interact with maize kinetochore protein CENH3. The Plant Cell **14**.